Materials Today Bio 26 (2024) 101100

Contents lists available at ScienceDirect

Materials Today Bio

journal homepage: www.journals.elsevier.com/materials-today-bio

Influence of physicochemical characteristics of calcium phosphate-based biomaterials in cranio-maxillofacial bone regeneration. A systematic literature review and meta-analysis of preclinical models

Ehsan Sadeghian Dehkord [a,b], Bruno De Carvalho [c,d], Marie Ernst [e], Adelin Albert [e,f], France Lambert [c,d,1], Liesbet Geris [a,b,g,*,1]

[a] GIGA In Silico Medicine, Biomechanics Research Unit (Biomech), University of Liège, Belgium
[b] Prometheus, The R&D Division for Skeletal Tissue Engineering, KU Leuven, Belgium
[c] Department of Periodontology, Oral-Dental and Implant Surgery, CHU of Liège, Belgium
[d] Dental Biomaterials Research Unit (d-BRU), University of Liège, Belgium
[e] Biostatistics and Research Method Center (B-STAT), CHU of Liège and University of Liège, Belgium
[f] Department of Public Health Sciences, University of Liège, Belgium
[g] Department of Mechanical Engineering, Biomechanics Section (BMe), KU Leuven, Belgium

ARTICLE INFO

Keywords:
Calcium phosphate
Biomaterials
Physicochemical
Cranio-maxillofacial
Intra-oral bone formation
Preclinical
Bone defect
Animal study
Bone regeneration
Bone scaffold

ABSTRACT

Objectives: Calcium phosphate-based biomaterials (CaP) are the most widely used biomaterials to enhance bone regeneration in the treatment of alveolar bone deficiencies, cranio-maxillofacial and periodontal infrabony defects, with positive preclinical and clinical results reported. This systematic review aimed to assess the influence of the physicochemical properties of CaP biomaterials on the performance of bone regeneration in preclinical animal models.

Methods: The PubMed, EMBASE and Web of Science databases were searched to retrieve the preclinical studies investigating physicochemical characteristics of CaP biomaterials. The studies were screened for inclusion based on intervention (physicochemical characterization and *in vivo* evaluation) and reported measurable outcomes.

Results: A total of 1532 articles were retrieved and 58 studies were ultimately included in the systematic review. A wide range of physicochemical characteristics of CaP biomaterials was found to be assessed in the included studies. Despite a high degree of heterogeneity, the meta-analysis was performed on 39 studies and evidenced significant effects of biomaterial characteristics on their bone regeneration outcomes. The study specifically showed that macropore size, Ca/P ratio, and compressive strength exerted significant influence on the formation of newly regenerated bone. Moreover, factors such as particle size, Ca/P ratio, and surface area were found to impact bone-to-material contact during the regeneration process. In terms of biodegradability, the amount of residual graft was determined by macropore size, particle size, and compressive strength.

Conclusion: The systematic review showed that the physicochemical characteristics of CaP biomaterials are highly determining for scaffold's performance, emphasizing its usefulness in designing the next generation of bone scaffolds to target higher rates of regeneration.

1. Introduction

Bone defects in the cranio-maxillofacial (CMF) region can be caused by injuries, cancerous bone resections, periodontal diseases, congenital disorders, and bone resorption following tooth extraction. They often require bone regeneration prior to or simultaneously to implant placement in order to restore deformities and the patient's functions [1–4]. Autologous bone graft procedures remain the clinical gold standard owing to the highest level of biological safety, biocompatibility, matched mechanical requirements and structural similarity in terms of

* Corresponding author. GIGA *In Silico* Medicine, Biomechanics Research Unit (Biomech), University of Liège, Belgium.
E-mail addresses: e.sadeghian@uliege.be (E. Sadeghian Dehkord), bruno.decarvalho@chuliege.be (B. De Carvalho), m.ernst@chuliege.be (M. Ernst), aalbert@uliege.be (A. Albert), france.lambert@chuliege.be (F. Lambert), liesbet.geris@kuleuven.be (L. Geris).
[1] France Lambert and Liesbet Geris contributed equally to this work and shared senior authorship.

https://doi.org/10.1016/j.mtbio.2024.101100
Received 21 March 2024; Received in revised form 20 May 2024; Accepted 21 May 2024
Available online 23 May 2024

growth factors and biomolecules for osteogenesis [5,6]. Nevertheless, autografts suffer multiple drawbacks such as limited availability, donor-site morbidity, high resorption rates and difficulty in shaping into desired geometries [7–10]. Tissue engineering (TE) using cell-based or growth factor strategies, usually combined with a carrier material, can be used to regenerate the defect site. The application of TE strategies is still limited in the clinic setting due to cost and tissue complexities in the CMF region. Moreover, TE strategies require cumbersome processes in laboratories [11]. Therefore, guided bone regeneration (GBR) combined with biomaterials has become an alternative used in periodontology, implantology and oral surgery for the regeneration of CMF bone defects [12–14]. This biomaterial-based strategy consists in implanting an acellular biodegradable scaffold that can recruit the necessary mesenchymal stem cells and/or osteoprogenitor cells from the surrounding tissues to regenerate the defect [15]. GBR solutions offer several potential advantages such as no restrictions on availability, reduced risk of immunoreactivity, fewer surgical complications as well as the possibility of tailoring the structure to regulate the bone formation microenvironment by manipulating the physicochemical specifications [16,17].

A wide variety of biomaterials have been utilized in CMF bone regeneration, belonging to different material classes and from different origins such as autografts, allografts, xenografts and alloplasts (synthetic biomaterials). Bioceramic materials comprise the majority of inorganic biomaterial scaffolds whereas biopolymers represent the majority of organic ones. While the ideal bone graft substitute should be accessible, economical and free of ethical and immunological issues with predictable handling, the morphological and physicochemical properties of biomaterials seem to play an important role in their regenerative performance as suggested by several authors [18–20]. Polymers like polylactic acid (PLA), polyglycolic acid (PGA), polycaprolactone (PCL), and methacrylates present advantages such as customizable forms, low immunogenicity, controllable resorbability, porosity, and tunable physiochemical properties [21,22]. These characteristics make them attractive for applications requiring tailored solutions and biocompatibility. Nevertheless, concerns persist regarding the release of acidic degradation byproducts, which can alter local pH levels and potentially hinder osteoconductivity. Additionally, these polymers may exhibit poor cell adhesion capacity, limiting their utility in certain dental procedures where robust tissue integration is crucial [23]. On the other hand, Metals such as nickel-titanium and magnesium-based bone substitutes offer desirable properties like osteoconduction, robust mechanical strength, and resistance to corrosion. These qualities support their effectiveness in providing structural support and promoting bone healing. However, their use may require surgical follow-ups and pose risks such as the possibility of soft tissue dehiscence [24]. CaP ceramics have demonstrated enhanced bone formation and the potential to serve as substitutes for bone grafting, thanks to their osteoconductive characteristics, resorbability, and outstanding biocompatibility [25,26]. Nevertheless, they may suffer from low mechanical adaptability such as brittleness, rapid resorption, and degradation [24].

In this systematic review, we focus on CaP-based biomaterials for CMF bone regeneration as this application domain presents its own unique challenges for bone regeneration that are not entirely overlapping with that of applications in the appendicular skeleton, as discussed above. Furthermore, as the addition of cells, coatings or growth factors alters the mechanism of action of bone regeneration in the biomaterial, and increases the cost of the implant, we focus on studies investigating the results of biomaterials-only strategies. The majority of CaP biomaterials currently used in clinical applications are of natural (human and animal) origin because of their similarities with natural bone structures. However, there is an increasing interest in the development and use of synthetic biomaterials in the clinic to increase safety (risk of disease transmission), ethics compliance and availability. The most widely used CaP biomaterials in CMF bone regeneration are based on hydroxyapatite (HAp), α and β-tricalcium phosphate (TCP) and/or biphasic calcium phosphate (BCP) [27]. However, synthetic biomaterials also present some limitations such as a lack of osteoconductivity or high resorption rates that might compromise the volumetric dimensions of the regenerated bone [28,29]. Given all this, producing optimized synthetic CaP biomaterials is crucially dependent on the fundamental understanding of the influence of the physicochemical biomaterial properties on the bone healing mechanisms [30] (Fig. 1).

This systematic review aimed to provide a comprehensive overview of the effect of the physicochemical properties of the CaP biomaterials on the biological performance of bone graft substitutes used for CMF bone regeneration or intra-oral bone augmentation in animal models. Following a well-documented approach, the current state of the art was assessed from reports published in the literature, and a meta-analysis was performed on the data extracted from these reports. The presented information can be used as input for the optimization of the structure and composition of future CaP biomaterials developments.

2. Material and methods

2.1. Study design

The present study was designed as a systematic literature review on the influence of physicochemical properties of CaP biomaterials implanted in cranio-maxillofacial bone defects. All studies involving the physicochemical characterization of CaP biomaterials and their *in vivo* evaluation in a cranio-maxillofacial animal model were assessed. The protocol for this review was registered with the international prospective register of systematic reviews (PROSPERO) with registration number CRD42019121604.

2.2. Focused question and search strategy

The systematic review was performed according to SYRCLE's (SYstematic Review Centre for Laboratory animal Experimentation) guidelines [31], and the focus question was: "What is the influence of different physicochemical characteristics of CaP biomaterials in the preclinical cranio-maxillofacial bone regeneration process?". An electronic search of the literature was run on November 14, 2023, in the following databases: PubMed (MEDLINE), EMBASE and Web of Science (all databases). Only articles in the English language were included without restrictions on the geographical area of the study. A detailed search strategy including all search terms and relationships between them (Table 1) was developed for PubMed and then adopted appropriately for EMBASE and Web of Science.

Eligibility was initially determined by reading the title and abstracts identified in each search. For this purpose, all references were imported into an Endnote X9 database. After eliminating the duplicates [32] and non-relevant ones, they were exported to an online webtool (Rayyan QCRI) to perform the screening. An Excel sheet with all references was generated from the database. The list of unique titles and abstracts was screened by two independent reviewers (ESD and BDC) to determine the eligibility of each study based on the inclusion and exclusion criteria described below. The two lists of selected references were then compared in the webtool, and all disagreements were solved by discussion, or if persistent, by a third reviewer (FL). For the potentially relevant publications, the full-text paper publication was collected and screened to check if all specified inclusion criteria were indeed met.

2.3. Inclusion/exclusion criteria

Studies were selected according to the inclusion and exclusion criteria specified in Table 2.

2.4. Data extraction

The data extraction started once the selection process was validated.

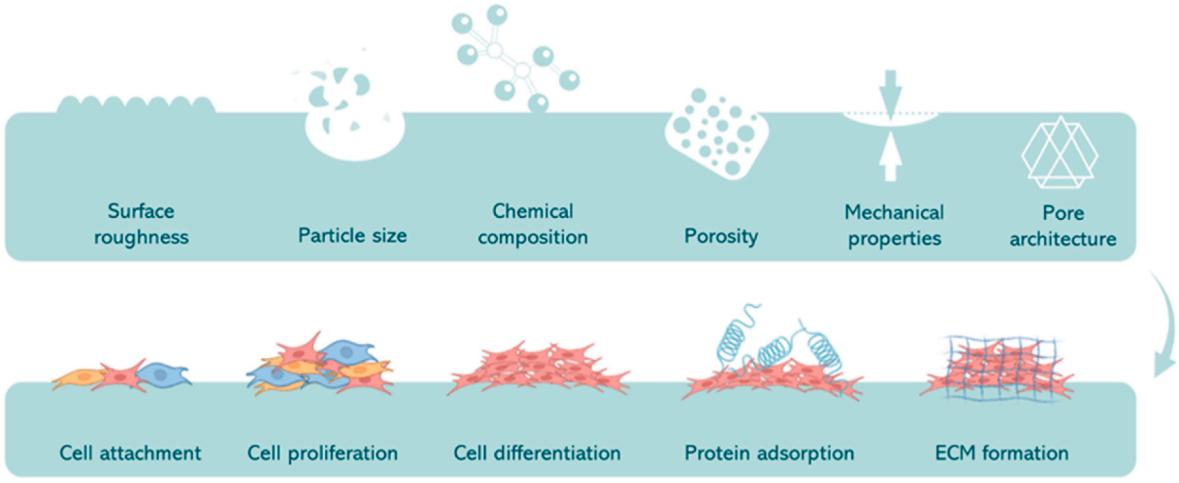

Fig. 1. An illustration of the key physicochemical properties influencing biological events. Biomaterials can manipulate molecular and cellular responses through their structural characteristics and composition (ECM: extracellular matrix).

Table 1
The search terms used in PubMed. [MeSH]: medical subject headings; [Supplementary concept]: terms in supplementary concept records (a thesaurus distinct from MeSH); [TIAB]: title/abstract terms.

Number	Search terms and combinations
#1	"calcium phosphate, dibasic, anhydrous" [Supplementary Concept] OR calcium-phosphate[TIAB] OR hydroxyapatite[TIAB] OR "Hydroxyapatites"[MeSH] OR "tricalcium phosphate" [Supplementary Concept] OR "beta-tricalcium phosphate" [Supplementary Concept] OR "hydroxyapatite-beta tricalcium phosphate" [Supplementary Concept] OR tricalcium-phosphate[TIAB]
#2	"Periodontal Atrophy"[MeSH] OR "guided tissue regeneration, periodontal"[MeSH] OR "alveolar ridge augmentation"[MeSH] OR "Parietal Bone/surgery"[MeSH] OR "Skull/drug effects"[MeSH] OR "Skull/injuries"[MeSH] OR "Skull Fractures"[MeSH] OR "Skull/surgery"[MeSH] OR maxillofacial injury[MeSH] OR periodontal-resorption[TIAB] OR Periodontal-Atrophy[TIAB] OR periodontal-guided-tissue-regeneration[TIAB] OR guided-bone-regeneration[TIAB] OR alveolar-bone*[TIAB] OR maxillofacial-bone-defect[TIAB] OR mandible-defect[TIAB] OR mandibular-bone-defect[TIAB] OR maxilla-defect [TIAB] OR maxillary-bone-defect[TIAB] OR maxillary-sinus-lift[TIAB] OR sinus-lift-model[TIAB] OR sinus-augmentation[TIAB] OR alveolar-ridge-augmentation[TIAB] OR skull-defect[TIAB] OR jaw-defect[TIAB] OR parietal-defect[TIAB] OR cranial-defect[TIAB] OR tooth-defect* [TIAB] OR calvarial-defect[TIAB] OR calvarial-defect[TIAB] OR calvarium-defect[TIAB] OR socket-preservation[TIAB] OR socket-grafting[TIAB] OR dental-socket*[TIAB]
#3	"Microscopy, Electron, Scanning"[MeSH] OR "X-Ray Diffraction"[MeSH] OR "Spectroscopy, Fourier Transform Infrared"[MeSH] OR "Microscopy, Scanning Tunneling"[MeSH] OR "Microscopy, Electron, Transmission"[MeSH] OR "Microscopy, Atomic Force"[MeSH] OR Brunauer–Emmett–Teller[TIAB] OR profilometr*[TIAB] OR X-Ray [TIAB] OR XRD[TIAB] OR ATM[TIAB] OR atomic-force-microscop* [TIAB] OR STM[TIAB] OR scanning-tunneling-microscop*[TIAB] OR scanning-tunnelling-microscop*[TIAB] OR FT-IR[TIAB] OR FTIR[TIAB] OR infrared-microscop*[TIAB] OR electron-microscop*[TIAB] OR electron-scanning-microscop*[TIAB] OR TEM[TIAB] OR SEM[TIAB] OR surface-roughness[TIAB] OR surface-propert*[TIAB] OR chemical-charact*[TIAB] OR chemical-propert*[TIAB] OR physical-charact* [TIAB] OR physical-propert*[TIAB] OR morphological-charact*[TIAB] OR morphological-propert*[TIAB] OR mechanical-charact*[TIAB] OR mechanical-propert*[TIAB]
#4	(#1) AND (#2) AND (#3)

Table 2
Preliminary inclusion and exclusion criteria used in this systematic review. PICOS is abbreviation of population, intervention, comparator, outcome, and study design.

PICOS	Inclusion criteria	Exclusion criteria
Population	All animals receiving a pure CaP biomaterial implant in periodontal and cranio-maxillofacial intra-bone defects induced by researchers	Human subjects, *in vitro* research, animals receiving implants in tissues other than cranio-maxillofacial bones, animals receiving implants that are not purely CaP biomaterials, animals receiving implants for bone defects that are not experimentally induced
Intervention	CaP biomaterial implants with distinct microstructural properties (particle size, porosity, pore size, mechanical properties, chemical composition, surface properties) in any physical form without tissue engineering or regenerative medicine approach (cell/drug/growth factor loaded)	All implants that are not CaP biomaterials, all implants that are not the only treatment in the defect site and have interference with other treatments, CaP biomaterial implants in the non-scaffold applications like coating, film, carrier, membrane etc.
Comparator	Not applicable	Not applicable
Outcome	Tissue regeneration responses (one or more) including newly formed bone (NB), bone to material contact (BMC), residual graft (RG)	None
Study design	*In vivo* experimental animal studies	Clinical trials, *in vitro* studies, reviews, case reports, observational research, uncontrolled studies

NB refers to the bone tissue that grows and integrates into the surface of the implanted bone biomaterial; BMC corresponds to the physical interaction between the host bone tissue and the implanted biomaterial; RG pertains to the remaining portion of the graft material that has not integrated with the surrounding bone tissue.

One reviewer (ESD) extracted the data from the included studies. The second reviewer (BDC) revised the extraction results to check the quality. Studies meeting the criteria for inclusion were read carefully to identify the following information: authors, title, year of publication, scaffold used in the study, scaffold's physical form, characterization methods, animal characteristics (species and numbers), bone defect model, duration of implantation, scaffold's physicochemical characteristics (primary outcomes), and tissue regeneration responses (secondary outcomes). The data were collected in an excel file. In case the information was not reported, the table entry was indicated as N/P (Not Provided).

2.5. Quality assessment and risk of bias

The methodological quality of the selected articles was assessed using the criteria outlined in the SYRCLE's Risk of Bias (RoB) tool which is specifically developed for animal studies [33]. The tool contains 10 entries that are related to selection bias, performance bias, detection bias, attrition bias, reporting bias and other biases. Following the signaling questions proposed by Hooijmans et al. (2014), the items in the RoB tool were scored as low risk, high risk or "unclear", the latter indicating that the item was not reported and, therefore, the risk of bias was unknown. Supplementary Table S1 presents the risks and how they were scored for RoB assessment. As animal studies are known for their poor reporting quality in comparison with randomized controlled trials, it is likely that many items of the RoB tool were not reported or poorly reported (Hooijmans et al.2014). Therefore, in addition to the RoB assessment, four indicators of methodological quality were checked. One overall study quality indicator (Q11 in Table S1) scored whether any randomization was reported for any level of the experiment. Likewise, we included two overall study quality indicators to acquire additional information on the reporting quality of the studies (Q12 & Q13 in Table S1). Specifically, the number of interventions for the animals and the number of animals to be analyzed for each time point were retrieved. In addition, we included a final study quality indicator related to how the outcomes were reported in different studies: quantitative numeric format versus qualitative (Q14 in Table S1). When study results were only available graphically, the item was scored "unclear". To extract data from graphs, WebPlotDigitizer was used (A. Rohatgi, https://automeris.io/WebPlotDigitizer, v4.7, 2024) was used. One reviewer (ESD) conducted the RoB and methodological quality assessment, and in case of doubt, a second reviewer (BDC) was consulted.

Prior to the meta-analysis, a descriptive review of the study characteristics was carried out. The meta-analysis was performed on a dataset including all covariates (quantitative physicochemical properties of biomaterials used in the studies) and outcome variables (NB, BMC, and RG).

2.6. Statistical methods

Each outcome variable Y (NB, BMC, or RG) was analyzed with respect to covariates available from N experimental samples (meta statistical units), each sample resulting from a clearly identified experiment conducted on a number (n) of animals over a certain time, whether published in the same paper or in different papers, whether involving the same animals or not. Results were expressed as mean, standard deviation (SD) and range for quantitative variables, while frequency tables (number and percent for each category) were used for categorical findings. In some cases, to avoid the influential effect of outliers or extreme values, the mean was replaced by the median and the standard deviation by a robust version $SD = 0.74 \times (P75 - P25)$, with P25 and P75, the 25th and 75th percentiles of the sample data, respectively. The Spearman correlation coefficient was used to quantify the association between the physicochemical characteristics of biomaterials. Agreement between reviewers was assessed by the Cohen kappa coefficient (κ). A log-transform was applied to some covariates to normalize their skewed distribution. Outcomes being expressed in percent, a logit transform was applied to normalize their distribution, specifically $Logit\ (Y) = \log [Y/(100 - Y)]$. Furthermore, outcome data being obtained from a varying number (n) of animals, a weight (w) was associated with each value as the inverse of their sampling variance ($SE^2 = SD^2/n$), provided SD and n were available; if not, w was estimated by regression and imputed from existing data. Lastly, since outcome data were not all statistically independent (some were correlated because repeated on the same animals), meta weighted generalized linear mixed effects models (W-GLMM) were used to estimate outcomes and assess the potential effect of covariates like time or type of biomaterial. All meta regression coefficient estimates were presented with their standard error and p-value. Results were considered significant at the 5 % critical level ($p < 0.05$). Calculations were performed using SAS (Version 9.4; Analytics Software and Solution, SAS Institute, Cary, North Carolina) and R (Version 3.6.1; R Foundation for Statistical Computing, Vienna).

3. Results

3.1. Systematic review and study data description

The initial literature search yielded 2103 potentially eligible articles. After removing the duplicates and the ones not in English, 1532 articles were screened in the subsequent process. Of this number, 1342 were excluded based on inclusion and exclusion criteria. The full text of 190 articles were assessed after which another 132 were excluded, resulting in 58 articles meeting the final inclusion/exclusion criteria. The inter-reviewer agreement was $\kappa = 0.92$ for titles and abstract evaluation and $\kappa = 0.89$ for full-text evaluation. The search strategy and retrieved articles are summarized in Fig. 2 and Table 3, the latter providing a summary of the study characteristics of the included publications. In 25 out of the 58 final included studies, HAp scaffolds were characterized and implanted; TCP scaffolds were used in 15 studies, BCP scaffolds in 24 studies, octacalcium phosphate (OCP)/amorphous calcium phosphate (ACP) and their combination in 2 studies, dicalcium phosphate (DCP) in one study and other types of CaPs in 2 studies (eggshell CaPs, respectively non-defined CaP). The scaffolds were implanted in the form of 3D rigid structures (disc, block, cylinder, cube, sponge, and tube) in 24 studies, non-rigid structures (granules, particles, spheres, and powder) in 32 studies, and aqueous structures (paste and injectable cement) in 2 studies. The actual physical form is provided in Table 3. In terms of animal models, there was substantial heterogeneity between studies with rats used in 23 out of 58 studies (for a total number of animals $n > 608$), rabbits in 20 studies ($n > 208$), dogs in 9 ($n > 67$), mini-pigs in 3 ($n = 19$), sheep in one ($n = 6$), mice in one ($n = 5$) and baboons in one ($n = 4$). Bone defect models were the typical defects used in CMF bone regeneration studies: calvarial defects (32 studies), mandibular defects (9), parietal defects (4), alveolar defects (4), sinus augmentation (2), skull defects (3), bilateral (maxilla and mandibular) defects (1), cranial defects (2) and mastoid obliteration (1). Outcomes were assessed over observation periods (time) ranging from 30 days to 40 weeks (Table 3).

Various types of physicochemical characteristics were recorded from various studies. Pore size and porosity were assessed in 29 studies ($N = 98$ experimental samples) and 24 studies ($N = 84$), respectively. Particle and granule sizes were reported in 23 studies ($N = 79$); 20 studies ($N = 53$) reported the composition of CaP used for their *in vivo* tests. XRD patterns were reported in 34 studies ($N = 105$) and FT-IR spectra in 12 studies ($N = 40$), confirming the chemical composition and phases of biomaterials. Surface properties were characterized in 12 studies ($N = 42$) and mechanical properties in 11 studies ($N = 30$). Ca/P ratio was reported in 6 studies ($N = 18$) and some other characteristics were reported less frequently: density (5 studies, $N = 9$), pore or void volume (4 studies), interconnectivity (2 studies), crystallinity (2 studies) and wall thickness (1 study). Thirty-nine studies reported bone regeneration responses in a quantitative way and the remaining 19 studies reported the responses qualitatively. Consequently, the meta-analysis was conducted on the 39 studies with quantitative outcomes. The outcome variables reported in these studies were distributed as follows: newly formed bone (38 studies, $N = 163$), residual graft (21 studies, $N = 80$) and bone to material contact (4 studies, $N = 31$). All the outcomes reported in the included articles are detailed in Table 3.

3.2. Quality assessment and risk of bias

Due to the insufficient number of reported items, the RoB and methodological quality assessments yielded many "unclear" scores, representing an unknown risk of bias (Fig. 3). The individual scores of the RoB tool and the methodological quality indicators of each included

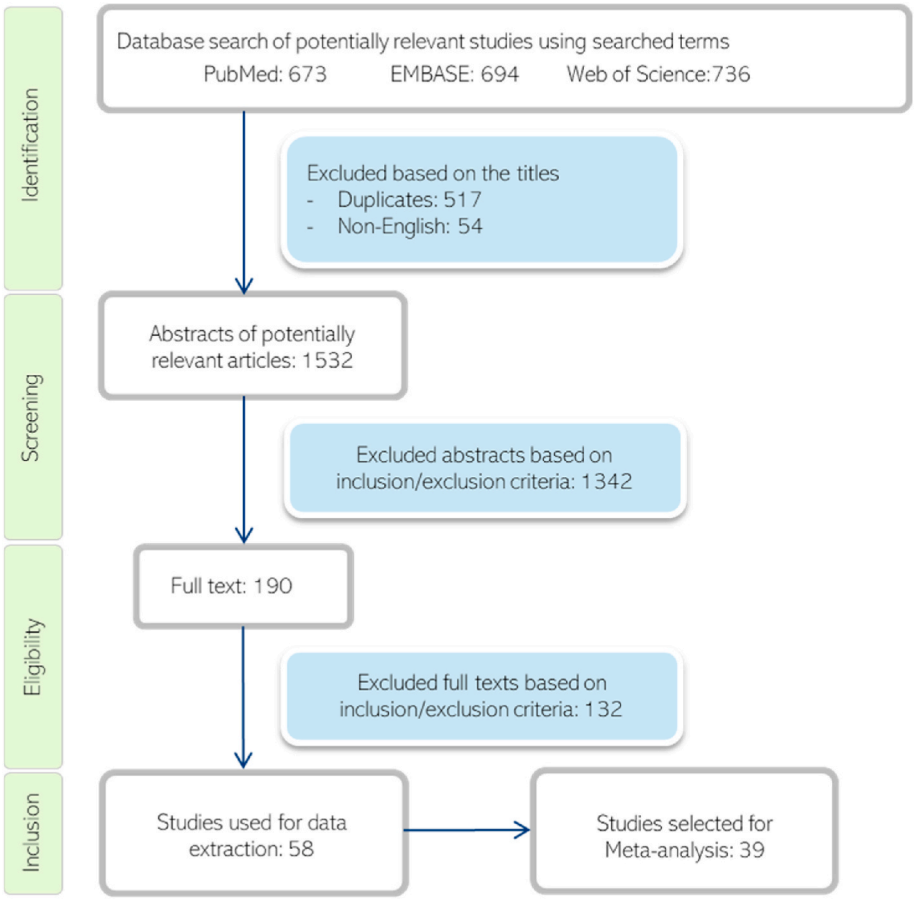

Fig. 2. Flow diagram for the review and selection process of studies included in the systematic review.

study are provided in Supplementary Table S2. Regarding selection bias (Fig. 3; Q1–Q3), the sequence generation process was reported in only one study (2 %; Q1), mentioning the use of software for group randomization (Calvo-Guirado et al., 2015). The randomization method was unclear in all other studies, however, many of them mentioned that the animals were randomly assigned to exposure groups. Baseline similarities were reported more often (41 %; Q2), whereas information about allocation concealment was not reported at all (Q3). Likewise, no study reported on random housing and blinding of caregivers (Q4 and Q5, respectively). As a result, performance bias could not be judged. With respect to detection bias (Q6 and Q7), no study described the random selection of animals for outcome assessment (Q6) and in only three studies (5 %; Q7) the outcome assessor for the histological assessment was reported to be blinded (Yang et al., 2014; Lim et al., 2015 and Mangano et al., 2015). Incomplete outcome data were adequately addressed in most of the included studies (89 %; Q8), resulting in a low attrition risk of bias for these studies. In the assessment of reporting bias (Q9), no study was found to have a high risk of bias. Other potential sources of bias were identified in one study (2 %; Q10) because of simultaneous additional implantations (Ripamonti et al., 2008). In addition to the risk of bias, four study quality indicators were used to assess the methodological quality of the studies. In 41 % of the studies, randomization at any level of the experiment was reported (Q11).

In all studies, the number of interventions on the animals was reported (Q12) and most of them reported the number of animals to be analyzed at each time point (89 %; Q13). Assessment of the outcomes revealed that 68 % of the studies reported the outcome in a numeric quantitative format, 15 % of them reported qualitatively and the remaining 17 % showed their results using graphs only (Q14).

3.3. Meta-analysis

The meta-analysis was based on N = 164 experimental samples, resulting from 73 animal experiments from 39 scientific articles, each experimental sample yielding at least one outcome value. NB was missing for one experimental sample (da Silva Brum et al., 2019), while BMC and RG were available for 31 and 80 experimental samples, respectively. Overall brute force mean ± SD (range) for NB values was 29.4 ± 22.6 % (1.6–95.5 %), for BMC values 45.3 ± 23.8 % (6.2–78.8 %), and for RG values 34.2 ± 17.3 % (4.6–91.5 %). Data for each outcome were widely dispersed which may be explained by the many factors characterizing the *in vivo* experiments discussed below. The distributions of all study characteristics employed in the meta-analysis are provided in Supplemental Table S3.

3.3.1. Analysis of new bone (NB)

Mean NB values were weighed by the inverse of their sampling variance, specifically by $w = n/SD^2$. Weights could not be calculated for 32 experimental samples (SD and/or n missing). Instead, they were estimated by regressing log(w) on logit(NB), namely $w = \exp\{-2.52 - 0.95 \log[NB/(100\text{-}NB)]\}$, as pictured in Supplemental Fig. S1. Indeed, a highly significant relationship was found between the two variables ($r = -0.65$, $p < 0.0001$). Five NB values (all <5 %) had extremely high weights ($w > 15$) compared to the other w-values (median ± robust SD of weights equal to 0.24 ± 0.41). These highly influential NB observations, respectively $w = 49.9$ and 15.9 (Xia et al., 2014), 15.9 (Yang et al., 2014), 33.3 and 30.8 (Intapibool et al., 2020), were ultimately discarded (see Supplemental Table S5), leaving 158 data points for the meta-analysis. A weighted generalized linear mixed model (W-GLMM) fitted to NB values alone (without covariates) yielded an estimated NB average

Table 3
Summary characteristics of the papers included in the systematic review. Papers with qualitative outcomes were not included in the meta-analysis. XRD: X-ray diffraction; SEM: scanning electron microscopy; AES: auger electron microscopy; IRRS: infrared reflection spectroscopy; FT-IR: Fourier-transform infrared spectroscopy; OM: optical microscopy; EDXA: energy dispersive X-ray analysis; FESEM: field-emission scanning electron microscopy; Mech: mechanical characterization; ICP-AES: Inductively coupled plasma atomic emission spectroscopy; BET: Brunauer–Emmett–Teller.

Paper ID	Biomaterial(s)	Physical form	Characterization methods	Characteristics	Animal	Qty.	Bone defect	Duration	Observation	Outcome
Abdel-Fattah et al. (1994) [34]	VHAP	Block	XRD	Diffraction pattern	Rabbit	6	Mandibular defect	3 months	Radiography SEM Infra-red spectral analysis	Bone healing Bone-implant integration Carbonate and phosphate resorption
Denissen et al. (1995) [35]	HAp	Tube	SEM, AES, XRD, IRRS	Particle diameter, diffraction pattern, absorbance spectra, surface area, Ca/P ratio	Dog	2	Mandibular defect	6 months	Radiography Histology	Interfaces observation Bone ingrowth
Roy et al. (2003) [36]	HAp-Ch HAp-No	Disk	Mercury porosimetry, XRD	Particle size, diffraction pattern, surface area, Ca/P ratio	New Zealand white rabbits	12	Mandibular defect	6 months	Histology Histomorphometry	New bone area(%) Linear ingrowth(%) Mineral apposition rate (um/day) continuity index
Fleckenstein et al. (2006) [37]	HAp/TCP	macroporous disk microporous disk granules	SEM	micro-pore size	Rat	33	calvarial defect	10 weeks	Histology Histomorphometry	New bone formation(%)
Suzuki et al. (2006) [38]	OCP Ca-deficient HAp (HL6h) Ca-deficient HAp (HL48h)	Granules	XRD, FT-IR	Diffraction pattern, absorbance spectra, surface area, chemical composition, Ca/P ratio	Rat	30	Calvaria defect	12 weeks	Histology Histomorphometry Radiography XRD	Newly formed bone(%) Structural changes
Simon et al. (2007) [39]	HAp(DW250S) HAp(DW250 M) HAp(DW250L) HAp(DW400S) HAp(DW400 M) HAp(DW400L)	Disc	OM, SEM	Void volume	New Zealand white rabbits	16	Calvarial defect	16 weeks	microCT radiography	Bone ingrowth volume (mm^3) Normalized bone ingrowth(%)
Park et al. (2008) [40]	BioOss Egg-shell(ES) ES-CaP-1 ES-CaP-2 ES-CaP-3	Granules	SEM, EDXA, XRD, FT-IR	Diffraction pattern, absorbance spectra, Ca/P ratio	Rat	30	Calvarial defect	8 weeks	Histology Histomorphometry	Newly formed bone area(%) Remaining bone graft particle area(%) BMC(%)
Ripamonti et al. (2008) [41]	HAp/β-TCP(19/81) HAp/β-TCP(4/96)	Disc	SEM, XRD, FT-IR	Macro and micro-pore size, diffraction pattern, absorbance spectra	Baboon	4	Calvarial defect	365 days	Histology Histomorphometry	Bone volume fraction (%) Matrix volume fraction (%) FVA (%)
Xu et al. (2008) [42]	β-TCP	Bulk	FESEM, XRD, Mech.	Porosity, Macro-pore size, diffraction pattern, compressive strength	Rabbit	12	Calvarial defect	16 weeks	Micro-CT Histology Histomorphometry	New bone(%) Residual material(%)
Appleford et al. (2009) [43]	Micro and Nano-HAp	Cylinder	SEM, XRD	Porosity	Dog	10	Mandibular defect	12 weeks	Micro-CT Histology Histomorphometry	Mineralized bone formation(%) Area of Total Tissue (%) Area of Mineralized Bone (%)BV/TV, BS/TV, BS/BV, Tb.N, Tb.Sb, Tb.Th
Hirota et al. (2009) [44]	β-TCP (OSferion®)	Granules	SEM	Particle size, porosity, Macro-pore size	Rat	10	Mandibular defect	5 weeks	Histology Histomorphometry	Bone formation rate(%) Amount of material(%)

(*continued on next page*)

Table 3 (*continued*)

Paper ID	Biomaterial(s)	Physical form	Characterization methods	Characteristics	Animal	Qty.	Bone defect	Duration	Observation	Outcome
										Material absorption rate (%)
Takahashi et al. (2009) [45]	TCP	Sponge	SEM	Macro-pore size	Dog	10	Mandibular defect	8 weeks	Histopathology	Average bone mass (center and top of cavity) (mm^2)
Wang et al. (2009) [46]	β-TCP	Cube	SEM	Porosity, Macro-pore size	Dog	4	Mandibular defect	24 weeks	Histomorphometry Radiography Sequential fluorescent labeling	Newly formed bone(%) Height and thickness of alveolar ridge bone (mm) Mineralization level(%)
Yao et al. (2009) [47]	BCP	Cylinder	SEM, XRD	Porosity, Macro and micro-pore size, chemical composition, mechanical properties	Dog	10	Mandibular defect	8 weeks	99mTc-MDP SPECT Mech. Pro analysis Histology	New bone filled
Park et al. (2010) [48]	CaP	Evacuated and filled microspheres	XRD, SEM	Particle size, diffraction pattern, wall thickness, evacuated area	New Zealand white rabbits	N/P	Calvarial defect	6 weeks	Histology	Bone formation
Park et al. (2010) [49]	n-BCP-1 n-BCP-2 MBCP Osteon Cerasorb Bio-Oss	Granules	SEM	Particle size, chemical composition	New Zealand white rabbits	20	Calvarial defect	8 weeks	Histology Histomorphometry	New bone(%)
Hung et al. (2011) [50]	PC-HAp/β-TCP, MBCP	Granules	SEM, XRD	Particle size, chemical composition, crystallite size	Dog	4	Bilateral maxilla and mandible defect	16 weeks	Histology Histomorphometry	New bone(%) Ratio of new bone formation
De Oliveira Lomelino et al. (2012) [51]	BCP	Granules	SEM, XRD, FT-IR	Particle size, diffraction pattern, absorbance spectra, chemical composition	Rat	10	Calvarial defect	45 days	Histology Histomorphometry	New bone tissue(%)
Klijn et al. (2012) [52]	CPC-IP	injectable cement	SEM, μCT, Gillmore test	Porosity, Chemical composition	Rat	12	Skull defect	12 weeks	Histology Histomorphometry	Newly formed bone(%) Appositional bone height(μm)
Lee et al. (2012) [53]	synthetic hydroxyapatite (sHA) eggshell hydroxyapatite (eHA)	Granules	FT-IR, XRD, SEM	Granule size, diffraction pattern, absorbance spectra	New Zealand white rabbits	16	Calvarial defect	8 weeks	Histomorphometry	Total new bone(%) Residual graft(%)
Cho et al. (2013) [54]	HAp	Granules	FESEM, XRD, EPMA, FT-IR,ICP-AES, ion chromatography	Particle size, diffraction pattern, absorbance spectra	New Zealand white rabbits	8	Calvarial defect	4 weeks	Histomorphometry	Newly formed bone(%) Implanted granule(%) Soft tissue(%)
Lee et al. (2013) [55]	60 TCP40HA	Granules	XRD, SEM	Porosity, Macro-pore size, diffraction pattern, chemical composition	Rat	52	Calvarial defect	8 weeks	Histology Micro-CT	BV/TV, BS/BV, Tb.Pf, SMI, Tb.Th, Tb.N, Tb.Sp, DA
Lee et al. (2013) [56]	HAp, β-TCP, BCP	Granules	XRD, SEM, FE-SEM, Micro-CT	Granule size, porosity, Macro-pore size, diffraction pattern, chemical composition, interconnectivity	Rat	130	Calvarial defect	8 weeks	Histology Micro-CT	BV/TV, BS/BV, Tb.Pf, SMI, Tb.Th, Tb.N, Tb.Sp, DA
Jang et al. (2014) [57]	HAps	Granules	SEM	Granule size	Rat	10	Mastoid obliteration	12 weeks	Fluorescent labeling Histology Micro-CT	Osteoconduction Ca deposition Resorption

(*continued on next page*)

Table 3 (*continued*)

Paper ID	Biomaterial(s)	Physical form	Characterization methods	Characteristics	Animal	Qty.	Bone defect	Duration	Observation	Outcome
Kobayashi et al. (2014) [58]	OCP ACPOCP/ACP	Granules	FT-IR, XRD, SEM	Granule size, diffraction pattern, absorbance spectra, chemical composition, Degree of Supersaturation	Rat	N/P	Calvarial defect	12 weeks	Radiography XRD Histology Histomorphometry	Radiopacity(%) New bone(%)
Lee et al. (2014) [59]	sHA eHA	Powder	FT-IR, XRD, SEM	Diffraction pattern, absorbance spectra	Rat	30	Parietal defect	8 weeks	Histomorphometry	Total new bone(%) Residual graft(%)
Xia et al. (2014) [60]	macroporous HAp	Block	SEM	Rod diameter, Macropore size and interconnected pore size	Rat	6	Calvarial defect	8 weeks	Micro-CT Histology Histomorphometry	BMD(mgHA/cm)Tb.Th (mm) New bone area(%) New vessel area(%)
Yang et al. (2014) [61]	β-TCP (Cerasorb), BCPs	Granules	SEM, XRD	Particle size, porosity, Macro and micro-pore size, diffraction pattern, chemical composition	New Zealand white rabbits	10	Calvarial defect	8 weeks	Histology Histomorphometry	Area of augmentation (mm^2) New bone area(mm^2,%) Residual particle area (mm^2,%)
Calasans-Maia et al. (2015) [62]	HAp and carbonated HAp	Spheres	SEM	SEM image	Rat	15	Alveolar defect	42 days	Histomorphometry	BV/TV(%)BiomatV/TV (%) RANKL(pg/mL) OPG(pg/mL)
Calvo-Guirado et al. (2015) [63]	BCP (4Bone®)	Granules	SEM	Granule size, Porosity, Macro and micro-pore size, chemical composition	New Zealand white rabbits	7	Parietal defect	12 weeks	Histomorphometry	Cortical Defect Closure (%) New bone(%) Connective tissue(%) Residual material(%)
Khan et al. (2015) [64]	BCP	Granules	helium pycnometry, Acoustic & electro-acoustic spectrometer	Particle size distribution, Chemical composition, Surface area, Density	New Zealand white rabbits	12	Parietal defect	8 weeks	Histomorphometry	Bone growth(%) Graft(%) Soft tissue(%)
Lim et al. (2015) [65]	BCPs	Block	XRD, SEM, Mech.	Porosity, Macro-pore size, Diffraction pattern, chemical composition, compressive strength, Crystalline phase (%)	New Zealand white rabbits	12	Calvarial defect	8 weeks	Histology Histomorphometry	Newly formed bone(%) Residual material(%)
Manchon et al. (2015) [66]	β-TCP	Granules	SEM, XRD, BET	Granule size, Porosity, pores fraction, pore size, diffraction pattern, surface area	New Zealand white rabbits	4	Calvarial defect	12 weeks	Histology Histomorphometry	New bone(%) Residual graft material (%) Fibrous tissue(%)
Manchon et al. (2015) [67]	β-TCP	Granules	SEM, XRD, BET	Porosity, pore size, pores fraction, diffraction pattern, surface area, blend composition, lattice parameters	New Zealand white rabbits	4	Parietal defect	12 weeks	Histology Histomorphometry	New bone(%) Residual graft material (%) Fibrous tissue(%)
Mangano et al. (2015) [68]	BCP	Block	SEM, XRD	Rod diameter, porosity, Macro and micro-pore size, chemical composition	Sheep	6	Sinus augmentation	90 days	Micro-CT Histology Histomorphometry	Newly deposited bone area/field area(%) peripheral and central
Lee et al. (2016) [69]	nano-sized β-TCP	Granules	SEM, XRD, FT-IR, BET, μCT, particle size analyzer, Mech.	Porosity, Macro-pore size, diffraction pattern, absorbance spectra, surface area, compressive strength	Dog	18	Mandibular defect	12 weeks	Histology	Newly formed bone(%) Residual quantity(%) Resorption(%)
Sheikh et al. (2016) [70]	dicalcium phosphate	Disc	SEM, XRD	Porosity, diffraction pattern, surface area, Ca/P ratio, Density, Compressive strength	New Zealand white rabbits	5	Calvarial defect	12 weeks	Histology Histomorphometry SEM XRD	Bone volume (%) Remaining graft(%)

(*continued on next page*)

Table 3 (*continued*)

Paper ID	Biomaterial(s)	Physical form	Characterization methods	Characteristics	Animal	Qty.	Bone defect	Duration	Observation	Outcome
Lambert et al. (2017) [71]	BHA (Bio-Oss) CBHA (Endobon) SHA (Osbone)	Granules	SEM, BET	Particle size, surface area	New Zealand white rabbits	24	Calvarial defect	12 weeks	Histology Histomorphometry	Newly formed bone(%) Biomaterial(%) BMC(%)
Diao et al. (2018) [72]	3D Plotted β-TCP	Paste	μCT, SEM, XRD	Porosity, Macro-pore size, Diffraction pattern, Connectivity	SD Rats	N/P	Calvarial defect	12 weeks	Micro-CT Histology Biomechanical	New bone(%) BMD(g.cm-3) BV(mm3) Max load(N) Stiffness(N/mm)
Fan et al. (2018) [73]	ABBM, BioOss	Granules	SEM, BET, XPS, XRD, FT-IR	Macro-pore size, Diffraction pattern, absorbance spectra, XPS spectrum, surface area, average pore volume	New Zealand white rabbits	16	Calvarial defect	12 weeks	Micro-CT Histology Histomorphometry	Newly formed bone(%) remnant graft(%)
Yao et al. (2018) [74]	BCPs	Block	SEM, XRD	Porosity, Macro-pore size, Diffraction pattern, Chemical composition	Dog	9	Bilateral alveolar ridges	12 weeks	Fluorescent dye labeling Histology Histomorphometry Spiral CT	New bone formation(%) Graft volume
Madhumathi et al. (2018) [75]	CDHA β-TCP CDHA/β-TCP	Granules	XRD, FT-IR, TEM	Diffraction pattern, surface area	Rat	12	Cranial defect	12 weeks	Micro-CT Histology Immunohistochemistry	total healing score
da Silva Brum et al. (2019) [76]	BCP	nano-particle	SEM, XRD, mercury intrusion porosimetry, helium gas pycnometry	Porosity, Macro-pore size, Diffraction pattern, Density	Rat	48	Calvarial defect	4 weeks	Histology Histomorphometry	Graft remaining particles area(%) Graft remaining particles number(%) New tissue area(%)
De Carvalho et al. (2019) [77]	Non-sintered HAP HAp sintered at 820 °C HAp sintered at 1200 °C	Granules	SEM, XRD, BET	Macro and micro-pore size, Diffraction pattern, Surface area, Pore volume	mini-pig	5	Alveolar defects	3 months	Histology Histomorphometry	Regenerated area Regeneration(%) Newly formed bone(%) Biomaterial(%) Soft tissue(%) Bone to material contact(%)
Park et al. (2019) [78]	β-TCPs(a,b,c,d)	Block	SEM	Porosity, Macro and micro-pore size	Rat	48	Calvarial defect	4 weeks	Micro-CT Histology Immunohistochemistry	New bone formation Osteoblastic differentiation Type I collagen
Zhang et al. (2019) [79]	HAp α-TCP β-TCP BCP (30 % β-TCP) BCP (70 % β-TCP)	Disc	SEM, XRD, Mech.	Diffraction pattern, Ca/P ratio, Compressive strength, Solubility	Dog	N/P	Skull defect	8 months	Histology	New bone regeneration Vascularization Bone resorption
Hung et al. (2019) [80]	BCP	Granules	SEM	Porosity, Macro-pore size, Chemical composition, Compressive strength, Density	mini-pig	6	Sinus augmentation	12 weeks	Micro-CT Histometry	New bone (%) Connective tissue (%) Residual particles (%) Bone density variables (BA/TA and BS/TV) Bone architecture variables (Tb.Th and Tb.N) Bone spacing variable (Po.(OP))
Chi et al. (2020) [81]	3D-HAp	Cylinder	SEM, Mech.	Pore size, Compressive modulus	Rat	6	Skull defect	12 weeks	Micro-CT Histometry	BV/TV(%), Tb.N, Tb.Sp, Tb.Th,

(*continued on next page*)

Table 3 (*continued*)

Paper ID	Biomaterial(s)	Physical form	Characterization methods	Characteristics	Animal	Qty.	Bone defect	Duration	Observation	Outcome
Jensen et al. (2020) [82]	TCP	Cylinder	XRD, Mech.	Pore size, Diffraction pattern, Compressive force	Mouse	5	Calvarial defect	8 weeks	Luciferase scanning histology	Implant surface with bone (%)
Intapibool et al. (2020) [83]	BCP(30% TCP70%HAP) BCP(70% TCP30%HAp)	Granules	SEM, XRD	Granules size, Diffraction pattern, Micro-pore size, Macro-pore size, Chemical composition	Pig	8	Calvarial defect	16 weeks	Histology Histomorphometry	New bone(%) Residual graft material (%) Bone to material contact(%)
Kiyochi et al. (2020) [84]	BCP	Disc	SEM, XRD, Mech., Micro-hardness	Diffraction pattern, Particle size, Density, Porosity, Vickers hardness, Compressive strength	Rat	35	Calvarial defect	60 days	SEM Histology	Bone mineralization Presence of blood vessels
De Oliveira Junior et al. (2021) [85]	BioOss, BCPs	Granules	SEM, BET	Pore volume, specific surface area	Rat	45	Calvarial defect	90 days	Histology Histomorphometry	Bone neoformation (μm^2)
Seo et al. (2021) [86]	BCPs	Granules	SEM	Pore diameter, porosity, chemical composition	Rabbit	6	Calvarial defect	8 weeks	Micro-CT Histometry	New bone formation (mm^3) Residual graft(mm^3)
Wang et al. (2021) [87]	HAp fiber, BioOss	Fiber, Granules	FE-SEM, XRD	Diffraction pattern, Particle diameter, Pore size	Rabbit	8	Cranial defect	8 weeks	Micro-CT Histometry	BV/TV(%) New bone area(mm^2) Residual graft(%)
Ghayor et al. (2022) [88]	HAp1100 HAp1200 HAp1300 HAp1400	Cube	SEM, Mech, Microporosity, BET	Grain size, surface area, Microporosity, Compressive strength	Rabbit	N/P	Calvarial defect	8 weeks	Histomorphometry	Bone regeneration(%)
Da Silva et al. (2023) [89]	BCP	Cylinder	XRD, SEM/EDS	Diffraction pattern, Chemical composition	Rat	25	Alveolar defect	120 days	Histology	Alveolar regeneration
Wu et al. (2023) [90]	BCPs	Disc	SEM, FT-IR, Mech.	Porosity	Rat	6	Calvarial defect	12 weeks	Micro-CT Histology	New bone area(%)BV/TV(%)
Youseflee et al. (2023) [91]	nHAp	Disc	FE-SEM, XRD	Diffraction pattern	Rat	5	Calvarial defect	45 days	Histopathology histomorphometry, Immunohistochemistry	Fibrous connective tissue(%) New bone formation(%) Angiogenesis(%)

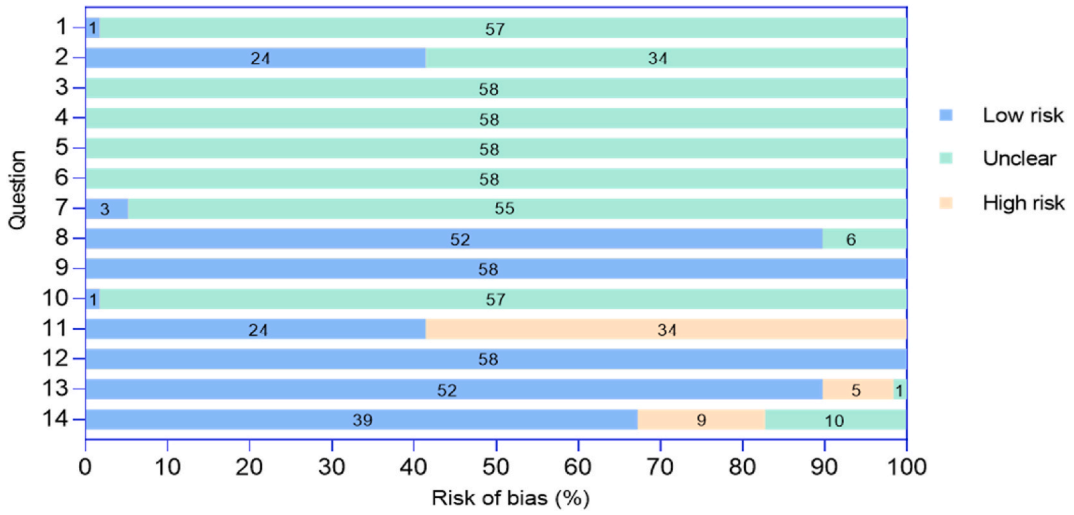

Fig. 3. Results of the risk of bias and methodological quality indicators for all included studies. The items in SYRCLE's Risk of Bias assessment; Questions Q1–Q10 were scored indicating a low or high risk of bias or were scored "unclear" when the item was not reported, resulting in an unknown risk of bias [33]. Questions Q11-Q14 are additional study quality indicators. For Q14, "low risk" indicates a numeric quantitative value was provided in the study, and a "high risk" indicates only qualitative results were reported. The label "unclear" was used for studies showing indicators only in graphical format. For additional information on the questions and indicators, see the methods section and Hooijmans et al. (2014).

of 11.4 %. Thus, when taking into consideration the statistical precision of NB values, the global mean was much lower than the one computed bluntly from all observations.

3.3.1.1. Effect of time. As displayed in Fig. 4, a highly significant relationship ($p < 0.0001$) was found between NB and time (*i.e.* the duration of the experiment expressed in days), and the estimated regression equation was Logit (NB) = −5.31 + 0.87 log(time). Thus, for an experiment duration of *e.g.* 50 days, the expected NB would be 12.9 %.

3.3.1.2. Biomaterials. The W-GLMM model evidenced significant differences of NB between biomaterials ($p = 0.0021$). The estimated NB values were low for HAp, TCP and BCP (8.6–13 %) and much higher for OCP-ACP-OA, DCP and CaP (25.7–39 %), but the latter were based on smaller sample sizes. Multiple comparisons showed significant difference between TCP and CaP ($p = 0.016$). When restricting the comparison of biomaterials to the first three types (HAp, TCP and BCP), significant differences were still detected ($p = 0.027$), the largest difference being between TCP and BCP (Supplemental Table S4). No interaction was found between biomaterials and time.

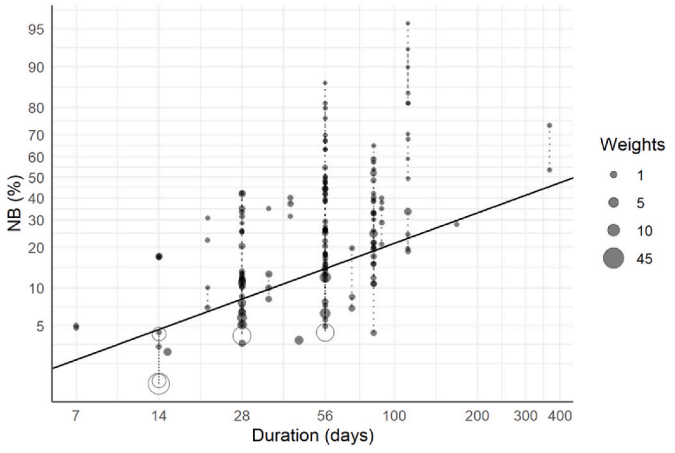

Fig. 4. Relationship between new bone NB (%) and duration of the animal experiment (log-scale) derived by weighted generalized linear mixed modeling. Five NB values with outlying weights (big hollow dots at days 14; 28 and 56) were eliminated from the analysis.

3.3.1.3. Experimental features. No significant association was found between NB and the number of implantations ($p = 0.56$), nor between NB and the physical form of the biomaterial ($p = 0.35$). By contrast, NB varied with the animal species used in the experiment ($p = 0.0025$), being 51.7 % for baboons, 10.6 % for dogs, 19.9 % for mini-pigs, 12.4 % for rabbits and 8.0 % for rats. The two latter species were also among the most used in the studies reported. NB values also differed significantly according to type of defect ($p < 0.0001$), being 9.6 % for calvarial defect (the most frequent, N = 131) and higher elsewhere but based on lower sample sizes: mandibular (N = 11, 10.4 %), alveolar (N = 6, 10.8 %), skull (N = 1, 10.8 %), sinus augmentation (N = 2, 25.4 %), cranial (N = 4, 41.1 %), parietal (N = 4, 47.2 %), and bilateral maxillary and mandibular defect (N = 4, 61.2 %). Estimated NB values (mean ± SE) with respect to the type of biomaterial, animal species and types of defects are displayed in Supplemental Fig. S2.

3.3.1.4. Biomaterial characteristics. When fitting W-GLMM to NB data according to each biomaterial characteristic, significant effects were observed for macropore size (N = 71, slope = −0.0016 ± 0.00031, $p < 0.0001$), and to a lesser extent to Ca/P ratio (N = 18, slope = −5.31 ± 2.33, $p = 0.041$) and to compressive strength (N = 20, slope = −0.11 ± 0.035, $p = 0.020$) (Fig. 5). The two first effects remained significant when including time in the regression analysis. Of note, no effect was observed for particle size (N = 79, $p = 0.85$), porosity (N = 74, $p = 0.13$), log-transformed micropore size (N = 27, $p = 0.64$), surface area (N = 32, $p = 0.18$), and density (N = 6, $p = 0.40$).

3.3.2. Analysis of bone to material contact (BMC)

BMC (%) was reported in only 4 papers involving 9 animal studies yielding a total of N = 31 experimental units. Weights could be calculated for all 31 BMC values, but one observation (Intapibool et al., 2020) was discarded due to an abnormally high weight (w = 20.8 compared to a median ± robust SD weight of 0.053 ± 1.74) (see Supplemental Table S5). Thus, 30 BMC values were used in the analysis. A W-GLMM was fitted to BMC values alone (without covariates) yielding an estimated BMC average of 34.1 %, lower than the value reported in Supplemental Table S3 based on all observations.

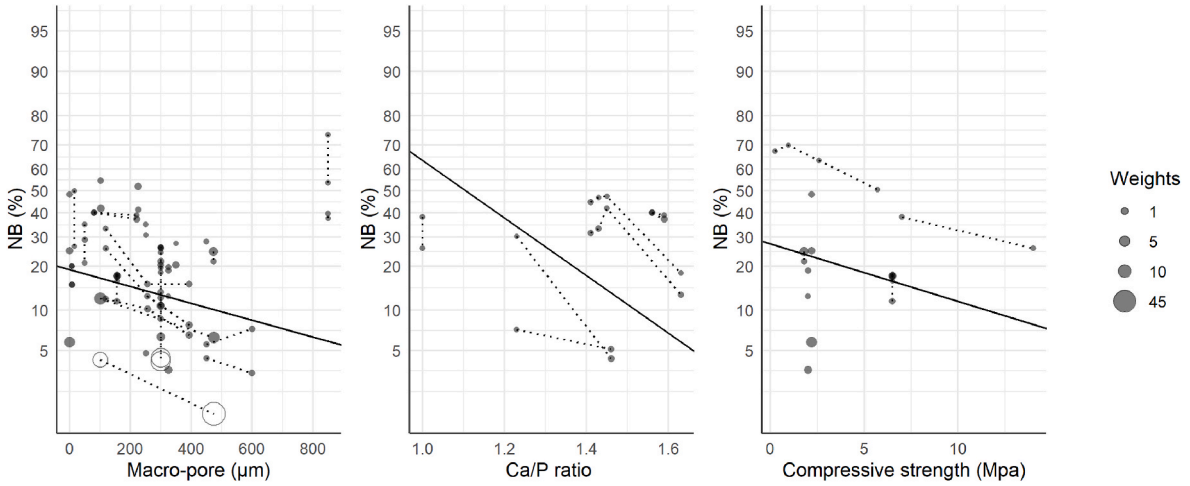

Fig. 5. Relationship between new bone (NB) and biomaterial characteristics (macropore size, Ca/P ratio and compressive strength respectively) derived by weighted generalized linear mixed modelling. NB values with outlying weights (big hollow dots) were eliminated from the analysis. Experimental samples data from the same animals are joined by dashed lines.

3.3.2.1. Effect of time. A time effect was evidenced by W-GLMM analysis (slope for log-transformed time equal to 1.53 ± 0.38, p = 0.0004) indicating that BMC values reported in the literature increased with respect to experiment duration (Fig. 6). The regression equation was: Logit (BMC) = - 6.88 + 1.53 log(duration). Thus, for an experiment duration of *e.g.* 50 days, the expected BMC would be 29 %.

3.3.2.2. Biomaterials. No difference was found in BMC values according to the three biomaterials utilized (p = 0.58), namely HAp (N = 11, 12.2 %), BCP (N = 12, 32.8 %) and CaP (N = 8, 68.6 %), as displayed in Fig. 7a.

Experimental features. A significant association was found between BMC and number of implantations (p < 0.0001), especially between 2 and 4 implantations (see Fig. 7b). By contrast, all BMC values were associated with non-rigid structures, and no significant association was detected between BMC and animal species (p = 0.97, mini-pig, rabbits, or rats), or between BMC and type of defect (p = 0.81 for alveolar or calvarial defects).

3.3.2.3. Biomaterial characteristics. When fitting W-GLMM to BMC data according to each biomaterial characteristic, significant effects were observed for the particle size (p < 0.0001, especially between 750 and 1500 μm), the Ca/P ratio (N = 8, slope = −12.3 ± 1.27, p < 0.0001) and to a lesser extent to surface area (N = 9, slope = 0.017 ± 0.0063, p = 0.042). Those three effects are illustrated in Fig. 8. Of note, no effect was observed for macropore size (N = 10, p = 0.86) nor for log-transformed micropore size (N = 10, p = 0.73); porosity was identical for all observations (N = 8, all 80 %) and there were no data on compressive strength nor density.

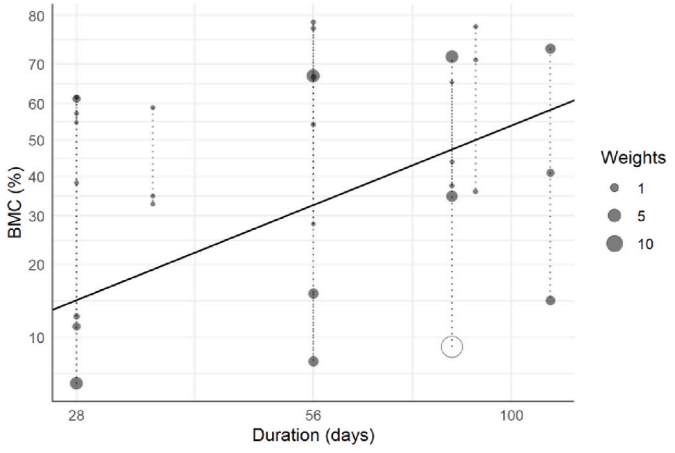

Fig. 6. Relationship between BMC (%) and duration of the animal experiment (log scale) derived by weighted generalized linear mixed modelling. One BMC value with outlying weight (big hollow dot at day 84) was eliminated from the analysis.

3.3.3. Analysis of residual graft (RG)

RG (%) was reported in 21 papers involving 43 animal studies yielding a total of N = 80 experimental units. Weights could be calculated for all RG values, but two observations (Yang et al., 2014 and Da Silva Brum et al., 2019) (Supplemental Table S5) had to be discarded because of an abnormally high weight (w = 11.5 and w = 84.9 compared to a median ± robust SD weight of 0.20 ± 0.41). Thus, 78 RG values were used in the meta-analysis. A weighted generalized linear mixed model (W-GLMM) was fitted to RG values alone (without covariates) yielding an estimated RG average of 20.1 %, much lower than the value reported before based on all observations.

3.3.3.1. Effect of time. No time effect could be evidenced by W-GLMM analysis (slope for log-transformed time is 0.37 ± 0.20, p = 0.067) indicating that RG values were relatively stable with respect to experiment duration.

3.3.3.2. Biomaterials. By contrast (Fig. 9a), significant RG differences were seen between biomaterials (p = 0.039); namely HAp (N = 22, 27.2 %), TCP (N = 15, 28.0 %), BCP (N = 33, 15.8 %), DCP (N = 2, 50.2 %) and CaP (N = 8, 24.7 %). When combining time and biomaterials, both effects became non-significant (p = 0.050 for biomaterial and p = 0.11 for time).

3.3.3.3. Experimental features. RG differed significantly according to several experimental features: physical form (p = 0.039) being 43.8 % for 3D rigid structures (N = 15) and 18.9 % for non-rigid structures (N = 65) (Fig. 9b); animal species (p = 0.022) being 40.9 % in dogs (N = 3) compared to 15.6 % in rabbits (N = 42), 18.3 % in rats (N = 17), 21.4 % in mini-pigs (N = 14) and 25.5 % in baboons (N = 4) (Fig. 9c). Interestingly, no significant association was detected between RG and the number of implantations (p = 0.080) neither between RG nor bone defects (p = 0.33).

3.3.3.4. Biomaterial characteristics. For biomaterial characteristics, only

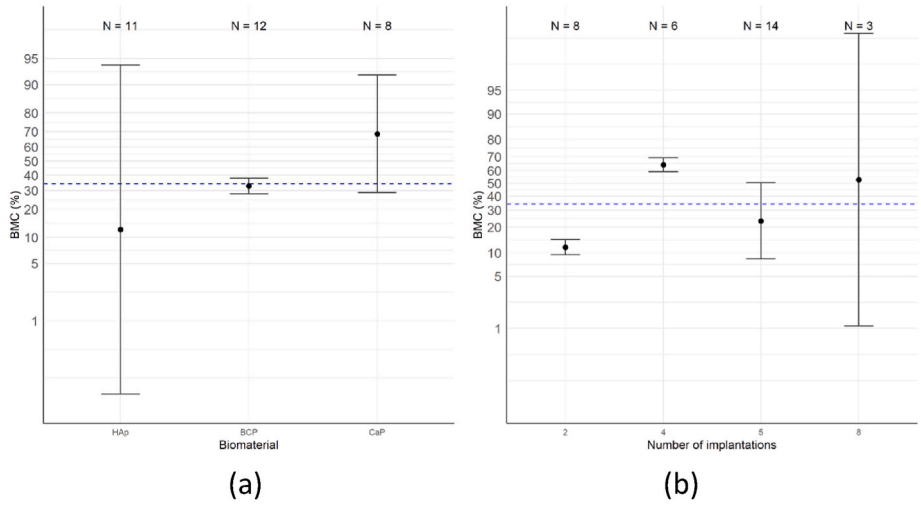

Fig. 7. Estimated bone to material contact (BMC) values (mean ± SE), globally (horizontal dotted lines) and with respect to (a) the biomaterials and (b) the number of implantations, as derived by weighted generalized linear mixed modelling.

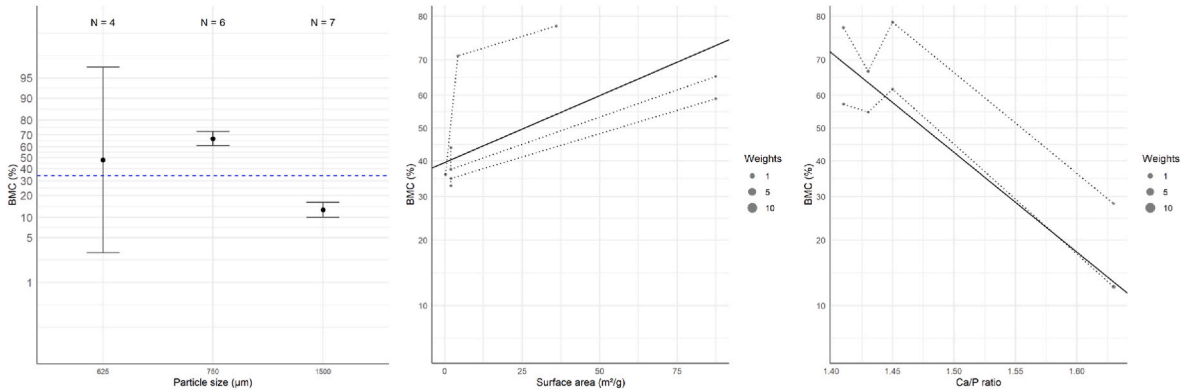

Fig. 8. Relationship between bone-material-contact (BMC) and characteristics (particle size, surface area and Ca/P ratio respectively) derived by weighted generalized linear mixed modeling. Experimental samples data from the same animals are joined by dashed lines.

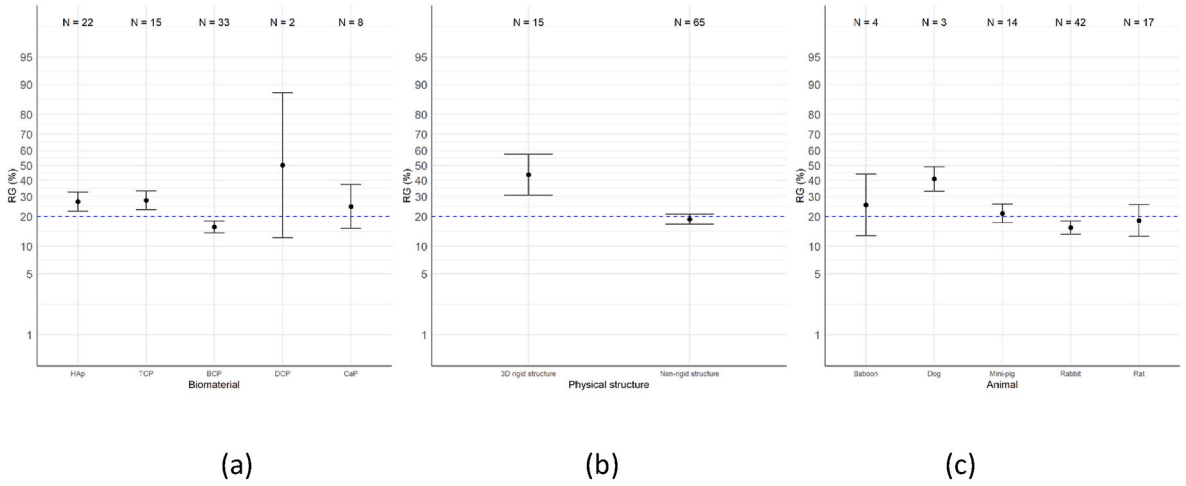

Fig. 9. Estimated residual graft (RG) values (mean ± SE), globally (horizontal dotted lines) and concerning (a) biomaterials, (b) physical structure and (c) animal species, as derived by weighted generalized linear mixed modeling.

macropore size (N = 44, slope = −0.0025 ± 0.00060, p = 0.0001), compressive strength (N = 16, slope = 0.13 ± 0.024, p = 0.0030) and particle size (N = 42, slope = 0.00089 ± 0.00034, = 0.016) were significantly associated with RG values.

3.4. Physicochemical characteristics of biomaterials

Spearman correlation analysis of the physicochemical characteristics of biomaterials exhibited perfect correlations between some of the

reported characteristics such as macropore size and Ca/P ratio ($r = +1$, $p < 0.0001$), macropore size and density ($r = -1$, $p < 0.0001$), and particle size and compressive strength ($r = +1$, $p < 0.0001$). The surface area was shown to have significant correlations with particle size ($r = +0.58$, $p = 0.028$), porosity ($r = -0.86$, $p = 0.0033$), macropore size ($r = +0.61$, $p = 0.022$), and Ca/P ratio ($r = +0.85$, $p = 0.0020$). A negative correlation was also found between macropore size and compressive strength ($r = -0.61$, $p = 0.022$). It should be noted that correlations were computed on small sample sizes and did not consider repeated observations. Correlations between all characteristics with an indication of the corresponding sample size are provided in Supplemental Table S6.

4. Discussion

The demand for technologies capable of enhancing the biomaterials used to treat CMF bone defects has been on the rise. This quest, accompanied by the advent of functionally tailored, biocompatible, and biodegradable materials, has motivated an enormous research interest in bone TE. As a result, different materials and fabrication methods have been investigated towards this end, leading to a deeper understanding of the geometrical, mechanical, and biological requirements associated with bone scaffolds. CaPs are a highly used scaffold material for bone regeneration because they actively promote osteogenesis. Structural control and optimization of CaPs in multi-scaled level may lead to significant developments in bone TE.

The aim of this study was to systematically review the preclinical *in vivo* evidence for the influence of biomaterial characteristics on CMF bone regeneration. Overall, the results of this systematic review and meta-analysis demonstrated that physicochemical characteristics of biomaterials influence bone regenerative responses; moreover, experimental features affect both the percentage of newly formed bone and the volume of the residual graft.

In some prior systematic reviews, the performance of bone tissue engineering scaffolds in *in vivo* animal models has been studied. In 2016, de Misquita et al. concluded that in the studies with calvarial bone defects, CaPs had important osteoinductive effects which increased when combined with other classes of biomaterials [92]. Their study aimed to determine which class of materials had achieved a higher rate of bone neoformation, so no correlation between the materials' properties and their regenerative capacity was developed. Additionally, in 2017, Shanbhag et al. conducted a systematic review of animal models to study how cell-based bone TE strategies enhance bone regeneration and/or biomaterial osteointegration in experimental peri-implant defects, compared to grafting with autogenous bone or only biomaterial scaffolds. They observed that bone regeneration and osseointegration in peri-implant defects were enhanced by the addition of osteogenic cells to biomaterial scaffolds [93].

To the best of our knowledge, the current study is the only systematic review and meta-analysis that has evaluated the effect of physicochemical characteristics of CaP biomaterials on CMF bone regeneration. To do so, we employed a comprehensive search and robust data assimilation procedure. For the 58 studies that were finally selected, a database was built based on the physicochemical characteristics of scaffolds and their bone regeneration capacity. The risk of bias (RoB) was assessed using SYRCLE's RoB tool. Each study was subjected to 10 questions related to the general risk of bias and 4 questions related to the quality of randomization and study item reporting. Meta-analysis was only performed for the 39 studies reporting quantitative outcomes. Our analysis of data from these studies demonstrates the impact of structural characteristics along with the experimental features on CMF bone regeneration.

4.1. Characteristics of animal models

Guidelines for designing preclinical animal models in bone TE have indicated some essential criteria as follows: (1) the models should match the clinical and biological environment and material formulation to the greatest extent possible; (2) they should allow the use of quantifiable parameters to evaluate success and functional performance of regenerated tissues; and (3) they should detect and predict clinically relevant differences in biological performance between the regenerative therapies assessed [94]. In the present study, all these experimental features were attentively observed and their effect on the regeneration outcomes was analyzed. The average time of implant placement within included studies was 83.6 ± 53.5 days. Although some studies with relatively long evaluation times (Ripamonti et al., 2008 and Zhang et al., 2019) were present among the included studies, additional long-term *in vivo* assessments are needed to ensure preclinical safety. In the present meta-analysis, a significant effect of time on new bone tissue formation was observed. Regarding the animal models, seven different species were used across the included studies and small animals composed most tested animals (66 % rats and 22.7 % rabbits). The remaining 11.3 % were large animals (dog, mini-pig, mouse, sheep and baboon). In general, large animals resemble the clinical conditions in bone TE better than small ones. This is due to similarities to the human bone in terms of composition and density [95]. Nevertheless, rodents are more frequently used for the assessment of bone biomaterials for CMF indications (and in general) as they are less costly and easier in housing. However, they are primarily being used for preliminary screenings followed by verification in large animals that are considered for the last phase of validating a new intervention [95,96]. Moreover, small rodents have a more controlled and clearer genetic background with less variation among individual animals requiring a lower number of experimental values to achieve statistically valid data [96,97]. Rabbits also have the advantages of small size and easy handling while achieving their skeletal maturity by 6 months of age allowing higher volumes of bone tissue to be formed in set-ups for testing periodontal and CMF reconstruction therapies. They also report higher reliability in terms of critical size defects [98].

4.2. Types of bone defects and biomaterials

Various types of defects, both acute and chronic, are studied in the CMF region. In this systematic review, 70.6 % of the included studies assessed cranial defects (calvarial, parietal and skull) and 29.4 % of them tested maxillo-facial ones (mandibular, alveolar, bilateral maxillomandibular and sinus augmentation). It should be remembered that the focus point in this review is the impact of physicochemical characteristics on the regeneration process. Therefore, only acute surgically created defects were studied here by excluding the defects with any factors interfering with bone regeneration. Likewise, for the biomaterial type, only pure CaP-based biomaterials free of any bioactive substances (cells, drugs, growth factors etc.) were included. This gives a better indication of how the physicochemical cues can affect the regeneration phase. There are some systematic reviews in which the implementation of cell-based approaches was studied in pre-clinical periodontal animal models [99–101]. A wide variety of biomaterial physical forms has been used in these bone defects. To avoid confusion due to the different terms used, they were grouped into three main categories. In total, 65.9 % of the biomaterials applied in the meta-analysis were non-rigid structures including granules, particles, spheres, and powder; 28 % were in 3D rigid forms including disc, block, cylinder, cube, sponge and tube; and 6.1 % were putties. Generally, the latter materials consist of a mixture of granules and an aqueous solution. They harden after *in situ* implantation or injection. The mechanical stability in these biomaterials is provided by the physical entanglement of CaP crystals. Their good handling and injectability extend their field of application, for instance for the treatment of bone fractures by minimally invasive techniques [102].

4.3. Outcome measures

Bone regenerative outcomes in this systematic review showed differences across all experimental circumstances mentioned above. Both

NB and BMC increased significantly over time. NB also differed notably among animal species and defect types. BMC was influenced by the number of implantations and physical form of biomaterials. RG was influenced significantly by biomaterial type, animal species and physical form. On the biomaterial type, the NB value for TCP was lower than for HAp and BCP while presenting the lowest RG in the meantime. Undoubtedly, the experimental variables documented across the studies included (such as biomaterial type, implantation time, number of implantations, animal species, defect type and biomaterial's physical form) have demonstrated varying degrees of influence on the regenerative outcomes.

It should be noted that BMC analysis allows the evaluation of the osteointegration and osteoconductive behavior of the bone substitutes and can be correlated to surface topography and/or to sintering temperatures used in the fabrication process. The manufacturing method of bone fillers allows for the preservation of a certain surface roughness favoring cell colonization, osteoconductivity and better bone regeneration [71,77]. High osteoconductive properties are important from a regenerative point of view since a tight network between bone and biomaterial plays a key role in implant primary stability and implant survival rates [71,103,104].

4.4. Influence of physicochemical characteristics on regenerative responses

A series of structural properties of CaPs have been analyzed within the regeneration process of included studies. Macropore size exhibited a significant effect on both NB and RG. The pore architecture at the macro and micro level affects the capability of the surrounding tissue to promote cell infiltration, migration, vascularization, and nutrient and oxygen flows [105]. The distribution of macropores in the included studies ranged from 0.4 μm to 850 μm and the ones of the micropores from 4 nm to 150 μm. These ranges are wider than what is usually suggested in the literature for successful bone regeneration (100–600 μm for macropores and micropores bigger than 20 nm) [105,106]. The significant effect of macro and micropore size on both NB and RG in the models developed here emphasizes the crucial role of porosity in the biomaterial's design regardless of the size. However, the issue remains for the optimal architecture of the pores in the structure. The presence of macropores favors osteointegration and angiogenesis while micropores increase the surface area available for protein adsorption [106]. It has been shown that the distribution of micropores on the walls of macropores could play a positive role in favoring the adsorption of proteins [107]. The pore size distribution was shown to influence the degradation performance of the scaffold, as shown here in RG values and, therefore, the biodegradation kinetics could be modulated by varying the pore architecture [108]. Another parameter that has mostly been dealt with in the included studies on non-rigid CaPs is particle size. This quantity varied from 0.5 μm to 1500 μm in the included articles and showed a significant effect on BMC and RG. Particle size was shown to be a highly determinant feature for the bioactivity of granulated CaPs that could be influenced by altering available surface area, roughness, mechanical performance and the resorbability of scaffolds [105].

Among the surface properties within the included studies, extensive attention has been directed toward the surface area, with ten studies spanning a wide range from 0.24 to 87.5 (m^2/g). This parameter plays a vital role in cellular attachment, offering ample anchoring sites for cell expansion and proliferation [109]. High surface areas exhibit a remarkable capability to absorb large quantities of biomolecules, thereby promoting extracellular responses [110]. The meta-analysis conducted herein elucidated a significant effect of surface area on BMC, emphasizing its crucial role in influencing cellular behaviors and material performance.

Mechanical properties were barely investigated in the included studies, and this is mainly because the CMF defects studied here were low or non-load bearing and did not require biomaterials matching the natural mechanical properties. Of note, the compressive modulus of sections of bone from the skull containing both cortical and cancellous regions is on the order of 0.36–5.6 GPa, depending on the direction of the load. These mechanical characteristics can be difficult to achieve with porous materials. CaPs may more easily approach these characteristics (though with lower toughness then native bone); however, it seems that such a high degree of mechanical competence is not necessarily needed (or even desirable) for bone repair [111].

Compressive strength is the most reported mechanical property in the literature as it is the dominant type of loading on BTE scaffolds in the body [112]. The compressive strength of various CaPs in the included studies varies from 1.8 MPa to 14 MPa and showed a significant effect on both NB and RG values. Nonetheless, mechanical properties can come with concerns in the CMF area when the implanted biomaterial does not fit the defect space. In the stiffer biomaterials, stress-shielding at the bone-material interface can cause greater bone loss and in the softer biomaterials, instability and limited motion can cause further damage [111]. One approach to overcome this issue is to employ *in situ* implantable CaPs that harden within the defect space [113,114].

Another physicochemical parameter that exhibited an impact on the regenerative responses of CaP biomaterials in the included studies is the Ca/P ratio. Overall, this ratio for CaP biomaterials used in biological applications can vary, depending on stoichiometry, from 1 to 1.67 for dicalcium phosphate (DCPA) and pure HAp, respectively. The values of almost the whole of this range have been extracted from the studies and then fed to the meta-analysis. The analysis showed a significant effect of the Ca/P ratio on NB and, to a lesser extent, on BMC. CaP biomaterials offer fast or slow degradation rates depending on their Ca/P molar ratio. β-TCP with a Ca/P ratio of 1.5 has been classified as a resorbable material while sintered HAp with a Ca/P ratio of 1.67 may show slower resorbability. Nevertheless, HAp becomes more resorbable in the presence of certain impurities, such as water-soluble binders and biodegradable polymers [115,116]. The other approach to increase HAp's resorbability is to reduce its grain size to nano-scale [117]. Hence, Ca/P ratio is a compositional parameter that is quite tunable for various functions. In some situations, fast resorbing materials with low mechanical properties are needed, therefore a lower ratio of Ca/P such as TCP is preferred. In other cases, materials in a higher ratio of Ca/P with more stability and slower resorption characteristics (*e.g.*, HAp) or a proper combination of both (TCP and HAp) are recommended.

Although the meta-analysis is able to extract quantified conclusions from the reviewed literature, the results do not permit going beyond establishing the general trends of influence of specific physicochemical parameters. The range of tested parameters are constrained by the choices made in the individual studies and often do not cover the entire parameter space. Furthermore, finding optimal properties also depends on the context of use for the biomaterial, requiring dedicated studies for each condition (*cfr* section on clinical relevance). For example, in a previously published study, we analyzed a series of in-house experiments performed in a rabbit sinus augmentation model, allowing us to use a different empirical model linking physicochemical biomaterial characteristics to intra-oral bone formation [118].

4.5. Limitations

One of the limitations of this systematic review is that only four studies have reported BMC. Additional data on this aspect would provide a more robust indication of how the experimental features and material characteristics interact with BMC. Likewise, some physicochemical characterizations were only scarcely investigated in the included studies, which limits interpreting their impact on the regeneration process. Mechanical properties were less thoroughly considered in the included studies, even though facial bones such as maxillary and mandible act as load-bearing bones for the dental region [119]. The mechanics of biomaterials are highly important for CMF defect treatments and future biomaterial developments should focus on this. These

considerations should not only include the stiffness difference between biomaterial and bone (potentially leading to stress shielding) but also the fixation of the biomaterial (avoiding movement) as well as ease of application. Other characteristics mostly neglected in the studies were surface energy, crystallinity and surface roughness. Surface roughness has a key role in protein adsorption [106], requiring further investigation in particular when the CaP biomaterials are implanted with biomacromolecules. Though there are studies that study these factors in detail, in this review we only selected studies that include an *in vivo* assessment. As a consequence, many of the selected studies had a focus that was not necessarily on the quantification of all the aforementioned physicochemical characteristics that have been shown to be. Finally, the meta-analysis was limited to the studies reporting the responses in a quantitative manner, so the studies using qualitative outputs were excluded from the analysis.

Despite searching for relevant studies in major electronic databases, we cannot rule out the possibility of missing studies. It should be noted as well that there was substantial heterogeneity across studies for all outcomes assessed, hence the results should be interpreted with caution. The study of applications combining scaffolds with cells, drugs or growth factors would be useful to elucidate how the structural elements should be tailored in their presence.

4.6. Clinical relevance

Systematic reviews and meta-analyses of animal studies can be useful for designing future clinical trials, capturing the underlying heterogeneity between studies and treatment effects, and improving the methodological quality of future studies [33]. The biomaterial design and selection for clinically successful CMF bone regeneration is fully dependent on the treatment strategy's requirements, emphasizing the role of biomaterial composition and physicochemical properties [120]. To test the efficacy and predictability of bone substitute materials, preclinical *in vivo* studies in clinically relevant animal models are a fundamental step in translational research [97,98,121]. Multiple experimental and preclinical studies demonstrate impressive results on bone neoformation in CaP scaffolds with a wide variety of characteristics [122,123], however, not all of them have exhibited similar efficacy in humans [124]. Developing statistical models for the meta-analysis of such studies, as done here for the preclinical models, will provide an indication of the most influencing elements to be considered in the early phases of biomaterial design. Future prospective randomized clinical trials should then be performed to identify clear indications in humans and to demonstrate clinical outcomes. The inherent limitation of preclinical modeling should always be considered while interpreting the results of the meta-analyses. In the context of *in vivo* experiments, the defects are usually surgically created and well controlled, with intact surrounding soft tissues and generally uncompromised blood supply, and most often in young and healthy animals. These conditions are often not present in clinical scenarios which may lead to the overestimation of clinical performance [94]. Therefore, the experimental defect models should be standardized in future preclinical investigations to better represent the clinical settings [125]. Moreover, in synthesizing the preclinical data encompassing regions from the cranium to the midface, mandibular bone, and the dento-alveolus, it is crucial to recognize inherent physiological, anatomical, and biomechanical distinctions within the human body. While the animal studies incorporated in this review predominantly focused on evaluating the regenerative potential of substitute materials, they did not sufficiently address the specific prerequisite characteristics crucial to each distinct region (*e.g.*, the use of animal cranial defect for human mandibular bone applications). Consequently, the outcomes were combined in a unified meta-analysis in the present study. Moving forward, it is imperative for future clinical studies to acknowledge and address these differences. The selection of biomaterials and their requisite characteristics should be tailored to meet the unique specifications of each region. Therefore, a strategic approach involving separate sub-analyses is warranted, ensuring a more refined understanding of the regenerative outcomes and paving the way for more targeted and effective clinical interventions.

5. Conclusion

This systematic review provides tangible evidence in support of the influence of fundamental and structural properties on the bone regenerative capacity of CaP biomaterials. Our findings from the included studies showed that macropore size, Ca/P ratio and compressive strength are influencing factors for newly formed bone in the regeneration process. Additionally, the contact between biomaterials and their surrounding tissue was notably influenced by particle size, Ca/P ratio and surface area. Regarding biodegradability, macropore size and compressive strength seemed to determine the amount of residual graft. Furthermore, the experimental setting is strongly determining the scaffold's performance. These observations may be useful in designing the next generation of bone scaffolds to target higher rates of regeneration. Additional investigations of CaP scaffolds in standardized preclinical studies could provide more insight into their fundamental features, promoting their application on a more regular basis and improving clinical outcomes.

CRediT authorship contribution statement

Ehsan Sadeghian Dehkord: Writing – review & editing, Writing – original draft, Methodology, Investigation, Data curation, Conceptualization. **Bruno De Carvalho:** Writing – review & editing, Investigation, Data curation. **Marie Ernst:** Writing – review & editing, Methodology, Investigation, Formal analysis. **Adelin Albert:** Writing – review & editing, Software, Methodology, Investigation, Formal analysis. **France Lambert:** Writing – review & editing, Supervision, Methodology, Funding acquisition, Conceptualization. **Liesbet Geris:** Writing – review & editing, Supervision, Resources, Project administration, Methodology, Funding acquisition, Conceptualization.

Declaration of competing interest

The authors declare the following financial interests/personal relationships which may be considered as potential competing interests: Liesbet Geris reports financial support was provided by European Research Council under the European Union's Horizon Europe programme/ERC Consolidator Grant No. 101088919. Liesbet Geris and France Lambert report financial support was provided by Walloon Region via the BIOWIN-BIOPTOS and Win2Wal-B2Bone projects. If there are other authors, they declare that they have no known competing financial interests or personal relationships that could have appeared to influence the work reported in this paper.

Data availability

This is a systematic review. All data is in the public domain and appropriately referenced.

Acknowledgments

This project received funding from the European Research Council under the European Union's Horizon Europe programme/ERC Consolidator Grant No. 101088919, and from the Walloon Region via the BIOWIN-BIOPTOS and Win2Wal-B2Bone project. We are grateful to Dr. Bert Avau (Centre for Evidence-Based Practice (CEBaP)) for his skillful support and assistance. We also acknowledge the kind support from Dr. Krizia Tuand and Dr. Kristel Paque (KU Leuven Bibliotheken).

Appendix A. Supplementary data

Supplementary data to this article can be found online at https://doi.org/10.1016/j.mtbio.2024.101100.

References

[1] Y. Kinoshita, H. Maeda, Recent developments of functional scaffolds for craniomaxillofacial bone tissue engineering applications, Sci. World J. 2013 (2013) 1–21, https://doi.org/10.1155/2013/863157.

[2] V. Fitzpatrick, Z. Martín-Moldes, A. Deck, R. Torres-Sanchez, A. Valat, D. Cairns, C. Li, D.L. Kaplan, Functionalized 3D-printed silk-hydroxyapatite scaffolds for enhanced bone regeneration with innervation and vascularization, Biomaterials 276 (2021) 120995, https://doi.org/10.1016/j.biomaterials.2021.120995.

[3] T.L. Aghaloo, P.K. Moy, Which hard tissue augmentation techniques are the most successful in furnishing bony support for implant placement? Int. J. Oral Maxillofac. Implants 22 (Suppl) (2007) 49–70.

[4] S. Jepsen, F. Schwarz, L. Cordaro, J. Derks, C.H.F. Hämmerle, L.J. Heitz-Mayfield, F. Hernández-Alfaro, H.J.A. Meijer, N. Naenni, A. Ortiz-Vigón, B. Pjetursson, G. M. Raghoebar, S. Renvert, I. Rocchietta, M. Roccuzzo, I. Sanz-Sánchez, M. Simion, C. Tomasi, L. Trombelli, I. Urban, Regeneration of alveolar ridge defects. Consensus report of group 4 of the 15th European workshop on periodontology on bone regeneration, J. Clin. Periodontol. (2019), https://doi.org/10.1111/jcpe.13121 jcpe.13121.

[5] M. Sanz, C. Dahlin, D. Apatzidou, Z. Artzi, D. Bozic, E. Calciolari, H. De Bruyn, H. Dommisch, N. Donos, P. Eickholz, J.E. Ellingsen, H.J. Haugen, D. Herrera, F. Lambert, P. Layrolle, E. Montero, K. Mustafa, O. Omar, H. Schliephake, Biomaterials and regenerative technologies used in bone regeneration in the craniomaxillofacial region: consensus report of group 2 of the 15th European Workshop on Periodontology on Bone Regeneration, J. Clin. Periodontol. 46 (2019) 82–91, https://doi.org/10.1111/jcpe.13123.

[6] V. Chappuis, L. Rahman, R. Buser, S.F.M. Janner, U.C. Belser, D. Buser, Effectiveness of contour augmentation with guided bone regeneration: 10-year results, J. Dent. Res. 97 (2018) 266–274, https://doi.org/10.1177/0022034517737755.

[7] G.F. Rogers, A.K. Greene, Autogenous bone graft: basic science and clinical implications, J. Craniofac. Surg. 23 (2012) 323–327, https://doi.org/10.1097/SCS.0b013e318241dcba.

[8] A. Sakkas, F. Wilde, M. Heufelder, K. Winter, A. Schramm, Autogenous bone grafts in oral implantology—is it still a "gold standard"? A consecutive review of 279 patients with 456 clinical procedures, Int. J. Implant Dent. 3 (2017) 23, https://doi.org/10.1186/s40729-017-0084-4.

[9] A. Ho-Shui-Ling, J. Bolander, L.E. Rustom, A.W. Johnson, F.P. Luyten, C. Picart, Bone regeneration strategies: engineered scaffolds, bioactive molecules and stem cells current stage and future perspectives, Biomaterials 180 (2018) 143–162, https://doi.org/10.1016/j.biomaterials.2018.07.017.

[10] M. Esposito, M.G. Grusovin, J. Rees, D. Karasoulos, P. Felice, R. Alissa, H. V. Worthington, P. Coulthard, Interventions for replacing missing teeth: augmentation procedures of the maxillary sinus, in: The Cochrane Collaboration (Ed.), Cochrane Database Syst. Rev., John Wiley & Sons, Ltd, Chichester, UK, 2010, p. CD008397, https://doi.org/10.1002/14651858.CD008397.

[11] L.N. Melek, Tissue engineering in oral and maxillofacial reconstruction, Tanta Dent. J. 12 (2015) 211–223, https://doi.org/10.1016/j.tdj.2015.05.003.

[12] A. Turri, I. Elgali, F. Vazirisani, A. Johansson, L. Emanuelsson, C. Dahlin, P. Thomsen, O. Omar, Guided bone regeneration is promoted by the molecular events in the membrane compartment, Biomaterials 84 (2016) 167–183, https://doi.org/10.1016/j.biomaterials.2016.01.034.

[13] B. Trajkovski, M. Jaunich, W.-D. Müller, F. Beuer, G.-G. Zafiropoulos, A. Houshmand, Hydrophilicity, viscoelastic, and physicochemical properties variations in dental bone grafting substitutes, Materials 11 (2018) 215, https://doi.org/10.3390/ma11020215.

[14] A. Kolk, J. Handschel, W. Drescher, D. Rothamel, F. Kloss, M. Blessmann, M. Heiland, K.-D. Wolff, R. Smeets, Current trends and future perspectives of bone substitute materials – from space holders to innovative biomaterials, J. Cranio-Maxillofac, Surgery (St Louis) 40 (2012) 706–718, https://doi.org/10.1016/j.jcms.2012.01.002.

[15] M.Á. Brennan, D.S. Monahan, B. Brulin, S. Gallinetti, P. Humbert, C. Tringides, C. Canal, M.P. Ginebra, P. Layrolle, Biomimetic versus sintered macroporous calcium phosphate scaffolds enhanced bone regeneration and human mesenchymal stromal cell engraftment in calvarial defects, Acta Biomater. 135 (2021) 689–704, https://doi.org/10.1016/j.actbio.2021.09.007.

[16] G. Thrivikraman, A. Athirasala, C. Twohig, S.K. Boda, L.E. Bertassoni, Biomaterials for craniofacial bone regeneration, Dent. Clin. 61 (2017) 835–856, https://doi.org/10.1016/j.cden.2017.06.003.

[17] J. Yun, J. Lee, C.W. Ha, S.J. Park, S. Kim, K. Koo, Y. Seol, Y. Lee, The effect of 3-D printed polylactic acid scaffold with and without hyaluronic acid on bone regeneration, J. Periodontol. 93 (2022) 1072–1082, https://doi.org/10.1002/JPER.21-0428.

[18] D.B. Bhuiyan, J.C. Middleton, R. Tannenbaum, T.M. Wick, Mechanical properties and osteogenic potential of hydroxyapatite-PLGA-collagen biomaterial for bone regeneration, J. Biomater. Sci. Polym. Ed. 27 (2016) 1139–1154, https://doi.org/10.1080/09205063.2016.1184121.

[19] X. Chen, H. Fan, X. Deng, L. Wu, T. Yi, L. Gu, C. Zhou, Y. Fan, X. Zhang, Scaffold structural microenvironmental cues to guide tissue regeneration in bone tissue applications, Nanomaterials 8 (2018) 960, https://doi.org/10.3390/nano8110960.

[20] H. Zhang, H. Zhang, Y. Xiong, L. Dong, X. Li, Development of hierarchical porous bioceramic scaffolds with controlled micro/nano surface topography for accelerating bone regeneration, Mater. Sci. Eng. C 130 (2021) 112437, https://doi.org/10.1016/j.msec.2021.112437.

[21] H.J. Haugen, S.P. Lyngstadaas, F. Rossi, G. Perale, Bone grafts: which is the ideal biomaterial? J. Clin. Periodontol. 46 (2019) 92–102, https://doi.org/10.1111/jcpe.13058.

[22] B. Sigusch, S. Kranz, A.C. Von Hohenberg, S. Wehle, A. Guellmar, D. Steen, A. Berg, U. Rabe, M. Heyder, M. Reise, Histological and histomorphometric evaluation of implanted photodynamic active biomaterials for periodontal bone regeneration in an animal study, Int. J. Mol. Sci. 24 (2023) 6200, https://doi.org/10.3390/ijms24076200.

[23] S.P. Pilipchuk, A.B. Plonka, A. Monje, A.D. Taut, A. Lanis, B. Kang, W. V. Giannobile, Tissue engineering for bone regeneration and osseointegration in the oral cavity, Dent. Mater. 31 (2015) 317–338, https://doi.org/10.1016/j.dental.2015.01.006.

[24] R. Zhao, R. Yang, P.R. Cooper, Z. Khurshid, A. Shavandi, J. Ratnayake, Bone grafts and substitutes in dentistry: a review of current trends and developments, Molecules 26 (2021) 3007, https://doi.org/10.3390/molecules26103007.

[25] R.A. Alsahafi, H.A. Mitwalli, A.A. Balhaddad, M.D. Weir, H.H.K. Xu, M.A.S. Melo, Regenerating craniofacial dental defects with calcium phosphate cement scaffolds: current status and innovative scope review, Front. Dent. Med. 2 (2021) 743065, https://doi.org/10.3389/fdmed.2021.743065.

[26] X. Gui, B. Zhang, Z. Su, Z. Zhou, Z. Dong, P. Feng, C. Fan, M. Liu, Q. Kong, C. Zhou, Y. Fan, X. Zhang, 3D-printed degradable hydroxyapatite bioactive ceramics for skull regeneration, MedComm – Biomater. Appl. 2 (2023) e41, https://doi.org/10.1002/mba2.41.

[27] W. Wang, K.W.K. Yeung, Bone grafts and biomaterials substitutes for bone defect repair: a review, Bioact. Mater. 2 (2017) 224–247, https://doi.org/10.1016/j.bioactmat.2017.05.007.

[28] A. Bruyas, F. Lou, A.M. Stahl, M. Gardner, W. Maloney, S. Goodman, Y.P. Yang, Systematic characterization of 3D-printed PCL/β-TCP scaffolds for biomedical devices and bone tissue engineering: influence of composition and porosity, J. Mater. Res. 33 (2018) 1948–1959, https://doi.org/10.1557/jmr.2018.112.

[29] R.S. Valtanen, Y.P. Yang, G.C. Gurtner, W.J. Maloney, D.W. Lowenberg, Synthetic and Bone tissue engineering graft substitutes: what is the future? Injury 52 (2021) S72–S77, https://doi.org/10.1016/j.injury.2020.07.040.

[30] M. Rahmati, E.A. Silva, J.E. Reseland, C.A. Heyward, H.J. Haugen, Biological responses to physicochemical properties of biomaterial surface, Chem. Soc. Rev. 49 (2020) 5178–5224, https://doi.org/10.1039/D0CS00103A.

[31] C.R. Hooijmans, K.E. Wever, R.B. de Vries, SYRCLE's starting guide for systematic reviews of preclinical animal interventions studies. https://www.radboudumc.nl/getmedia/4b1cbcb8-d9b6-45d5-b9fe-c92e43ab1dd4/SYRCLE-starting-guide-tool.aspx, 2016.

[32] W.M. Bramer, D. Giustini, G.B. De Jonge, L. Holland, T. Bekhuis, De-duplication of database search results for systematic reviews in EndNote, J. Med. Libr. Assoc. 104 (2016), https://doi.org/10.5195/jmla.2016.24.

[33] C.R. Hooijmans, M.M. Rovers, R.B. de Vries, M. Leenaars, M. Ritskes-Hoitinga, M. W. Langendam, SYRCLE's risk of bias tool for animal studies, BMC Med. Res. Methodol. 14 (2014) 43, https://doi.org/10.1186/1471-2288-14-43.

[34] W.I. Abdel-Fattah, W.G. Osiris, S.S. Mohamed, M.R. Khalil, Reconstruction of resected mandibles using a hydroxyapatite veterinary bone graft, Biomaterials 15 (1994) 609–614, https://doi.org/10.1016/0142-9612(94)90211-9.

[35] H. Denissen, W. Kalk, E. Van Beek, C. Löwik, S. Papapoulos, A. Van Den Hooff, Composites of hydroxyapatite and bisphosphonate: properties and alveolar bone response, J. Mater. Sci. Mater. Med. 6 (1995) 35–40, https://doi.org/10.1007/BF00121245.

[36] T. Dutta Roy, J.L. Simon, J.L. Ricci, E.D. Rekow, V.P. Thompson, J.R. Parsons, Performance of hydroxyapatite bone repair scaffolds created via three-dimensional fabrication techniques, J. Biomed. Mater. Res. 67A (2003) 1228–1237, https://doi.org/10.1002/jbm.a.20034.

[37] K.B. Fleckenstein, M.F. Cuenin, M.E. Peacock, M.A. Billman, G.D. Swiec, T. B. Buxton, B.B. Singh, J.C. McPherson, Effect of a hydroxyapatite tricalcium phosphate alloplast on osseous repair in the rat calvarium, J. Periodontol. 77 (2006) 39–45, https://doi.org/10.1902/jop.2006.77.1.39.

[38] O. Suzuki, S. Kamakura, T. Katagiri, M. Nakamura, B. Zhao, Y. Honda, R. Kamijo, Bone formation enhanced by implanted octacalcium phosphate involving conversion into Ca-deficient hydroxyapatite, Biomaterials 27 (2006) 2671–2681, https://doi.org/10.1016/j.biomaterials.2005.12.004.

[39] J.L. Simon, S. Michna, J.A. Lewis, E.D. Rekow, V.P. Thompson, J.E. Smay, A. Yampolsky, J.R. Parsons, J.L. Ricci, In vivo bone response to 3D periodic hydroxyapatite scaffolds assembled by direct ink writing, J. Biomed. Mater. Res. 83A (2007) 747–758, https://doi.org/10.1002/jbm.a.31329.

[40] J.-W. Park, S.-R. Bae, J.-Y. Suh, D.-H. Lee, S.-H. Kim, H. Kim, C.-S. Lee, Evaluation of bone healing with eggshell-derived bone graft substitutes in rat calvaria: a pilot study, J. Biomed. Mater. Res. 87A (2008) 203–214, https://doi.org/10.1002/jbm.a.31768.

[41] U. Ripamonti, P.W. Richter, R.W.N. Nilen, L. Renton, The induction of bone formation by *smart* biphasic hydroxyapatite tricalcium phosphate biomimetic matrices in the non-human primate *Papio ursinus*, J. Cell Mol. Med. 12 (2008) 2609–2621, https://doi.org/10.1111/j.1582-4934.2008.00312.x.

[42] S. Xu, K. Lin, Z. Wang, J. Chang, L. Wang, J. Lu, C. Ning, Reconstruction of calvarial defect of rabbits using porous calcium silicate bioactive ceramics,

Biomaterials 29 (2008) 2588–2596, https://doi.org/10.1016/j.biomaterials.2008.03.013.
[43] M.R. Appleford, S. Oh, N. Oh, J.L. Ong, In vivo study on hydroxyapatite scaffolds with trabecular architecture for bone repair, J. Biomed. Mater. Res. 89A (2009) 1019–1027, https://doi.org/10.1002/jbm.a.32049.
[44] M. Hirota, Y. Matsui, N. Mizuki, T. Kishi, K. Watanuki, T. Ozawa, T. Fukui, S. Shoji, M. Adachi, Y. Monden, T. Iwai, I. Tohnai, Combination with allogenic bone reduces early absorption of .BETA.-tricalcium phosphate (.BETA.-TCP) and enhances the role as a bone regeneration scaffold. Experimental animal study in rat mandibular bone defects, Dent. Mater. J. 28 (2009) 153–161, https://doi.org/10.4012/dmj.28.153.
[45] K. Takahashi, Effect of new bone substitute materials consisting of collagen and tricalcium phosphate, Bull. Tokyo Dent. Coll. 50 (2009) 1–11, https://doi.org/10.2209/tdcpublication.50.1.
[46] S. Wang, Z. Zhang, J. Zhao, X. Zhang, X. Sun, L. Xia, Q. Chang, D. Ye, X. Jiang, Vertical alveolar ridge augmentation with β-tricalcium phosphate and autologous osteoblasts in canine mandible, Biomaterials 30 (2009) 2489–2498, https://doi.org/10.1016/j.biomaterials.2008.12.067.
[47] J. Yao, X. Li, C. Bao, H. Fan, X. Zhang, Z. Chen, A novel technique to reconstruct a boxlike bone defect in the mandible and support dental implants with *In vivo* tissue-engineered bone, J. Biomed. Mater. Res. B Appl. Biomater. 91B (2009) 805–812, https://doi.org/10.1002/jbm.b.31459.
[48] J.-S. Park, S.-J. Hong, H.-Y. Kim, H.-S. Yu, Y.I. Lee, C.-H. Kim, S.-J. Kwak, J.-H. Jang, J.K. Hyun, H.-W. Kim, Evacuated calcium phosphate spherical microcarriers for bone regeneration, Tissue Eng. 16 (2010) 1681–1691, https://doi.org/10.1089/ten.tea.2009.0624.
[49] J.-W. Park, E.-S. Kim, J.-H. Jang, J.-Y. Suh, K.-B. Park, T. Hanawa, Healing of rabbit calvarial bone defects using biphasic calcium phosphate ceramics made of submicron-sized grains with a hierarchical pore structure, Clin. Oral Implants Res. 21 (2010) 268–276, https://doi.org/10.1111/j.1600-0501.2009.01846.x.
[50] C.-L. Hung, J.-C. Yang, W.-J. Chang, C.-Y. Hu, Y.-H. Lin, C.-H. Huang, C.-C. Chen, S.-Y. Lee, N.-C. Teng, In vivo graft performance of an improved bone substitute composed of poor crystalline hydroxyapatite based biphasic calcium phosphate, Dent. Mater. J. 30 (2011) 21–28, https://doi.org/10.4012/dmj.2010-060.
[51] R. de Oliveira Lomelino, I.I. Castro-Silva, A.B.R. Linhares, G.G. Alves, S.R. de Albuquerque Santos, V.S. Gameiro, A.M. Rossi, J.M. Granjeiro, The association of human primary bone cells with biphasic calcium phosphate (βTCP/HA 70:30) granules increases bone repair, J. Mater. Sci. Mater. Med. 23 (2012) 781–788, https://doi.org/10.1007/s10856-011-4530-1.
[52] R.J. Klijn, J.J.J.P. van den Beucken, R.P. Félix Lanao, G. Veldhuis, S. C. Leeuwenburgh, J.G.C. Wolke, G.J. Meijer, J.A. Jansen, Three different strategies to obtain porous calcium phosphate cements: comparison of performance in a rat skull bone augmentation model, Tissue Eng. 18 (2012) 1171–1182, https://doi.org/10.1089/ten.tea.2011.0444.
[53] S.-W. Lee, S.-G. Kim, C. Balázsi, W.-S. Chae, H.-O. Lee, Comparative study of hydroxyapatite from eggshells and synthetic hydroxyapatite for bone regeneration, Oral Surg. Oral Med. Oral Pathol. Oral Radiol. 113 (2012) 348–355, https://doi.org/10.1016/j.tripleo.2011.03.033.
[54] J.S. Cho, H.-S. Kim, S.-H. Um, S.-H. Rhee, Preparation of a novel anorganic bovine bone xenograft with enhanced bioactivity and osteoconductivity, J. Biomed. Mater. Res. B Appl. Biomater. 101B (2013) 855–869, https://doi.org/10.1002/jbm.b.32890.
[55] J.H. Lee, M.Y. Ryu, H.-R. Baek, K.M. Lee, J.-H. Seo, H.-K. Lee, Fabrication and evaluation of porous beta-tricalcium phosphate/hydroxyapatite (60/40) composite as a bone graft extender using rat calvarial bone defect model, Sci. World J. 2013 (2013) 1–9, https://doi.org/10.1155/2013/481789.
[56] J.H. Lee, M.Y. Ryu, H.-R. Baek, K.M. Lee, J.-H. Seo, H.-K. Lee, H.-S. Ryu, Effects of porous beta-tricalcium phosphate-based ceramics used as an E. coli-derived rhBMP-2 carrier for bone regeneration, J. Mater. Sci. Mater. Med. 24 (2013) 2117–2127, https://doi.org/10.1007/s10856-013-4967-5.
[57] C.H. Jang, Y.B. Cho, C.H. Choi, Y.S. Jang, W.-K. Jung, J.K. Lee, Comparision of osteoconductivity of biologic and artificial synthetic hydroxyapatite in experimental mastoid obliteration, Acta Otolaryngol. 134 (2014) 255–259, https://doi.org/10.3109/00016489.2013.859397.
[58] K. Kobayashi, T. Anada, T. Handa, N. Kanda, M. Yoshinari, T. Takahashi, O. Suzuki, Osteoconductive property of a mechanical mixture of octacalcium phosphate and amorphous calcium phosphate, ACS Appl. Mater. Interfaces 6 (2014) 22602–22611, https://doi.org/10.1021/am5067139.
[59] S.-W. Lee, C. Balázsi, K. Balázsi, D. Seo, H.S. Kim, C.-H. Kim, S.-G. Kim, Comparative Study of hydroxyapatite prepared from seashells and eggshells as a bone graft material, Tissue Eng. Regen. Med. 11 (2014) 113–120, https://doi.org/10.1007/s13770-014-0056-1.
[60] L. Xia, K. Lin, X. Jiang, B. Fang, Y. Xu, J. Liu, D. Zeng, M. Zhang, X. Zhang, J. Chang, Z. Zhang, Effect of nano-structured bioceramic surface on osteogenic differentiation of adipose derived stem cells, Biomaterials 35 (2014) 8514–8527, https://doi.org/10.1016/j.biomaterials.2014.06.028.
[61] C. Yang, O. Unursaikhan, J.-S. Lee, U.-W. Jung, C.-S. Kim, S.-H. Choi, Osteoconductivity and biodegradation of synthetic bone substitutes with different tricalcium phosphate contents in rabbits: bone Regeneration of Synthetic Bone Graft Material, J. Biomed. Mater. Res. B Appl. Biomater. 102 (2014) 80–88, https://doi.org/10.1002/jbm.b.32984.
[62] M.D. Calasans-Maia, B.R. de Melo, A.T.N.N. Alves, R.F. de B. Resende, R.S. Louro, S.C. Sartoretto, J.M. Granjeiro, G.G. Alves, Cytocompatibility and biocompatibility of nanostructured carbonated hydroxyapatite spheres for bone repair, J. Appl. Oral Sci. 23 (2015) 599–608, https://doi.org/10.1590/1678-775720150122.
[63] J.L. Calvo-Guirado, M. Garces, R.A. Delgado-Ruiz, M.P. Ramirez Fernandez, E. Ferres-Amat, G.E. Romanos, Biphasic β-TCP mixed with silicon increases bone formation in critical site defects in rabbit calvaria, Clin. Oral Implants Res. 26 (2015) 891–897, https://doi.org/10.1111/clr.12413.
[64] R. Khan, L. Witek, M. Breit, D. Colon, N. Tovar, M.N. Janal, R. Jimbo, P. G. Coelho, Bone regenerative potential of modified biphasic graft materials, Implant Dent. (2015), https://doi.org/10.1097/ID.0000000000000220. Publish Ahead of Print.
[65] H.-C. Lim, K.-H. Song, H. You, J.-S. Lee, U.-W. Jung, S.-Y. Kim, S.-H. Choi, Effectiveness of biphasic calcium phosphate block bone substitutes processed using a modified extrusion method in rabbit calvarial defects, J. Periodontal Implant Sci. 45 (2015) 46, https://doi.org/10.5051/jpis.2015.45.2.46.
[66] A. Manchón, M. Alkhraisat, C. Rueda-Rodriguez, J. Torres, J.C. Prados-Frutos, A. Ewald, U. Gbureck, J. Cabrejos-Azama, A. Rodriguez-González, E. López-Cabarcos, Silicon calcium phosphate ceramic as novel biomaterial to simulate the bone regenerative properties of autologous bone: silicon Calcium Phosphate Ceramic as Novel Biomaterial, J. Biomed. Mater. Res. 103 (2015) 479–488, https://doi.org/10.1002/jbm.a.35196.
[67] A. Manchón, M. Hamdan Alkhraisat, C. Rueda-Rodriguez, J.C. Prados-Frutos, J. Torres, J. Lucas-Aparicio, A. Ewald, U. Gbureck, E. López-Cabarcos, A new iron calcium phosphate material to improve the osteoconductive properties of a biodegradable ceramic: a study in rabbit calvaria, Biomed. Mater. 10 (2015) 055012, https://doi.org/10.1088/1748-6041/10/5/055012.
[68] C. Mangano, B. Barboni, L. Valbonetti, P. Berardinelli, A. Martelli, A. Muttini, R. Bedini, S. Tetè, A. Piattelli, M. Mattioli, In vivo behavior of a custom-made 3D synthetic bone substitute in sinus augmentation procedures in sheep, J. Oral Implantol. 41 (2015) 240–250, https://doi.org/10.1563/AAID-JOI-D-13-00053.
[69] D. Lee, Y. Pai, S. Chang, D. Kim, Microstructure, physical properties, and bone regeneration effect of the nano-sized β-tricalcium phosphate granules, Mater. Sci. Eng., C 58 (2016) 971–976, https://doi.org/10.1016/j.msec.2015.09.047.
[70] Z. Sheikh, J. Drager, Y.L. Zhang, M.-N. Abdallah, F. Tamimi, J. Barralet, Controlling bone graft substitute microstructure to improve bone augmentation, Adv. Healthcare Mater. 5 (2016) 1646–1655, https://doi.org/10.1002/adhm.201600052.
[71] F. Lambert, M. Bacevic, P. Layrolle, P. Schüpbach, P. Drion, E. Rompen, Impact of biomaterial microtopography on bone regeneration: comparison of three hydroxyapatites, Clin. Oral Implants Res. 28 (2017) e201–e207, https://doi.org/10.1111/clr.12986.
[72] J. Diao, J. OuYang, T. Deng, X. Liu, Y. Feng, N. Zhao, C. Mao, Y. Wang, 3D-Plotted beta-tricalcium phosphate scaffolds with smaller pore sizes improve in vivo bone regeneration and biomechanical properties in a critical-sized calvarial defect rat model, Adv. Healthcare Mater. 7 (2018) 1800441, https://doi.org/10.1002/adhm.201800441.
[73] Y.-P. Fan, J.-F. Lu, A.-T. Xu, F.-M. He, Physiochemical characterization and biological effect of anorganic bovine bone matrix and organic-containing bovine bone matrix in comparison with Bio-Oss in rabbits, J. Biomater. Appl. 33 (2018) 566–575, https://doi.org/10.1177/0885328218804926.
[74] J. Yao, H. Chen, Q. Gao, Z. Liang, Evaluation of osteoinductive calcium phosphate ceramics repairing alveolar cleft defects in dog model, Bio Med. Mater. Eng. 29 (2018) 229–240, https://doi.org/10.3233/BME-171725.
[75] K. Madhumathi, Y. Rubaiya, M. Doble, R. Venkateswari, T.S. Sampath Kumar, Antibacterial, anti-inflammatory, and bone-regenerative dual-drug-loaded calcium phosphate nanocarriers—in vitro and in vivo studies, Drug Deliv. Transl. Res. 8 (2018) 1066–1077, https://doi.org/10.1007/s13346-018-0532-6.
[76] I. da Silva Brum, J.J. de Carvalho, J.L. da Silva Pires, M.A.A. de Carvalho, L.B. F. dos Santos, C.N. Elias, Nanosized hydroxyapatite and β-tricalcium phosphate composite: physico-chemical, cytotoxicity, morphological properties and in vivo trial, Sci. Rep. 9 (2019) 19602, https://doi.org/10.1038/s41598-019-56124-4.
[77] B. De Carvalho, E. Rompen, G. Lecloux, P. Schupbach, E. Dory, J.-F. Art, F. Lambert, Effect of sintering on in vivo biological performance of chemically deproteinized bovine hydroxyapatite, Materials 12 (2019) 3946, https://doi.org/10.3390/ma12233946.
[78] M. Park, G. Lee, K. Ryu, W. Lim, Improvement of bone formation in rats with calvarial defects by modulating the pore size of tricalcium phosphate scaffolds, Biotechnol. Bioproc. Eng. 24 (2019) 885–892, https://doi.org/10.1007/s12257-019-0248-6.
[79] B. Zhang, H. Sun, L. Wu, L. Ma, F. Xing, Q. Kong, Y. Fan, C. Zhou, X. Zhang, 3D printing of calcium phosphate bioceramic with tailored biodegradation rate for skull bone tissue reconstruction, Bio-Des, Man (Lond.) 2 (2019) 161–171, https://doi.org/10.1007/s42242-019-00046-7.
[80] C. Hung, E. Fu, H. Chiu, H. Liang, Bone formation following sinus grafting with an alloplastic biphasic calcium phosphate in Lanyu Taiwanese mini-pigs, J. Periodontol. 91 (2020) 93–101, https://doi.org/10.1002/JPER.17-0748.
[81] H. Chi, G. Chen, Y. He, G. Chen, H. Tu, X. Liu, J. Yan, X. Wang, 3D-HA scaffold functionalized by extracellular matrix of stem cells promotes bone repair, Int. J. NANOMEDICINE 15 (2020) 5825–5838, https://doi.org/10.2147/IJN.S259678.
[82] M.B. Jensen, C. Slots, N. Ditzel, S. Kolstrup, M. Kassem, T. Thygesen, M. Ø. Andersen, Treating mouse skull defects with 3D-printed fatty acid and tricalcium phosphate implants, J. Tissue Eng. Regen. Med. 14 (2020) 1858–1868, https://doi.org/10.1002/term.3146.
[83] P. Intapibool, N. Monmaturapoj, K. Nampuksa, K. Thongkorn, P. Khongkhunthian, Bone regeneration of a polymeric sponge technique-Alloplastic bone substitute materials compared with a commercial synthetic bone material (MBCP+TM technology): a histomorphometric study in porcine skull, Clin. Exp. Dent. Res. 7 (2021) 726–738, https://doi.org/10.1002/cre2.394.

[84] H. de J. Kiyochi Junior, A.G. Candido, T.G.M. Bonadio, J.A. da Cruz, M.L. Baesso, W.R. Weinand, L. Hernandes, In vivo evaluation of interactions between biphasic calcium phosphate (BCP)-niobium pentoxide (Nb(2)O(5)) nanocomposite and tissues using a rat critical-size calvarial defect model, J. Mater. Sci. Mater. Med. 31 (2020) 71, https://doi.org/10.1007/s10856-020-06414-5.
[85] J.M. de Oliveira Junior, P.G. Montagner, R.C. Carrijo, E.F. Martinez, Physical characterization of biphasic bioceramic materials with different granulation sizes and their influence on bone repair and inflammation in rat calvaria, Sci. Rep. 11 (2021) 4484, https://doi.org/10.1038/s41598-021-84033-y.
[86] S.-J. Seo, Y.-G. Kim, Improved bone regeneration using collagen-coated biphasic calcium phosphate with high porosity in a rabbit calvarial model, Biomed. Mater. Bristol Engl. 16 (2020) 015012, https://doi.org/10.1088/1748-605X/abb1fc.
[87] F. Wang, H. Nakata, X. Sun, W.M. Maung, M. Sato, K. Kon, K. Ozeki, R. Ikumi, S. Kasugai, S. Kuroda, A novel hydroxyapatite fiber material for the regeneration of critical-sized rabbit calvaria defects, Dent. Mater. J. 40 (2021) 964–971, https://doi.org/10.4012/dmj.2020-327.
[88] C. Ghayor, I. Bhattacharya, J. Guerrero, M. Oezcan, F. Weber, 3D-Printed HA-based scaffolds for bone regeneration: microporosity, osteoconduction and osteoclastic resorption, Materials 15 (2022), https://doi.org/10.3390/ma15041433.
[89] C. da Silva, D. Scatolim, A. Queiroz, F. de Almeida, E. Volnistem, M. Baesso, W. Weinand, L. Hernandes, Alveolar regeneration induced by calcium phosphate ceramics after dental avulsion: study in young rats, Mater. Chem. Phys. 295 (2023), https://doi.org/10.1016/j.matchemphys.2022.127082.
[90] Y. Wu, Q. Cao, Y. Wang, Y. Liu, X. Xu, P. Liu, X. Li, X. Zhu, X. Zhang, Optimized fabrication of DLP-based 3D printing calcium phosphate ceramics with high-precision and low-defect to induce calvarial defect regeneration, Mater. Des. 233 (2023), https://doi.org/10.1016/j.matdes.2023.112230.
[91] P. Youseflee, F.E. Ranjbar, M. Bahraminasab, A. Ghanbari, D.R. Faradonbeh, S. Arab, A. Alizadeh, V.T. Nooshabadi, Exosome loaded hydroxyapatite (HA) scaffold promotes bone regeneration in calvarial defect: an in vivo study, Cell Tissue Bank. 24 (2023) 389–400, https://doi.org/10.1007/s10561-022-10042-4.
[92] M.R.D.O.F. de Misquita, R. Bentini, F. Goncalves, The performance of bone tissue engineering scaffolds in *in vivo* animal models: a systematic review, J. Biomater. Appl. 31 (2016) 625–636, https://doi.org/10.1177/0885328216656476.
[93] S. Shanbhag, N. Pandis, K. Mustafa, J.R. Nyengaard, A. Stavropoulos, Alveolar bone tissue engineering in critical-size defects of experimental animal models: a systematic review and meta-analysis: alveolar bone tissue engineering in critical-size defects, J. Tissue Eng. Regen. Med. 11 (2017) 2935–2949, https://doi.org/10.1002/term.2198.
[94] G.F. Muschler, V.P. Raut, T.E. Patterson, J.C. Wenke, J.O. Hollinger, The design and use of animal models for translational research in bone tissue engineering and regenerative medicine, Tissue Eng., Part B 16 (2010) 123–145, https://doi.org/10.1089/ten.teb.2009.0658.
[95] J. Aerssens, S. Boonen, G. Lowet, J. Dequeker, Interspecies differences in bone composition, density, and quality: potential implications for in vivo bone research, Endocrinology 139 (1998) 663–670, https://doi.org/10.1210/endo.139.2.5751.
[96] A. Stavropoulos, A. Sculean, D.D. Bosshardt, D. Buser, B. Klinge, Pre-clinical in vivo models for the screening of bone biomaterials for oral/craniofacial indications: focus on small-animal models, Periodontol 68 (2015) (2000) 55–65, https://doi.org/10.1111/prd.12065.
[97] G. Pellegrini, Y.J. Seol, R. Gruber, W.V. Giannobile, Pre-clinical models for oral and periodontal reconstructive therapies, J. Dent. Res. 88 (2009) 1065–1076, https://doi.org/10.1177/0022034509349748.
[98] S. Stübinger, M. Dard, The rabbit as experimental model for research in implant dentistry and related tissue regeneration, J. Invest. Surg. 26 (2013) 266–282, https://doi.org/10.3109/08941939.2013.778922.
[99] X.-Z. Yan, F. Yang, J.A. Jansen, R.B.M. de Vries, J.J.J.P. van den Beucken, Cell-based approaches in periodontal regeneration: a systematic review and meta-analysis of periodontal defect models in animal experimental work, Tissue Eng., Part B 21 (2015) 411–426, https://doi.org/10.1089/ten.teb.2015.0049.
[100] S.A. Tassi, N.Z. Sergio, M.Y.O. Misawa, C.C. Villar, Efficacy of stem cells on periodontal regeneration: systematic review of pre-clinical studies, J. Periodontal. Res. 52 (2017) 793–812, https://doi.org/10.1111/jre.12455.
[101] S. Portron, A. Soueidan, A.-C. Marsden, M. Rakic, C. Verner, P. Weiss, Z. Badran, X. Struillou, Periodontal regenerative medicine using mesenchymal stem cells and biomaterials: a systematic review of pre-clinical studies, Dent. Mater. J. 38 (2019) 867–883, https://doi.org/10.4012/dmj.2018-315.
[102] M. Bohner, Resorbable biomaterials as bone graft substitutes, Mater, Today Off. 13 (2010) 24–30, https://doi.org/10.1016/S1369-7021(10)70014-6.
[103] L. Molly, H. Vandromme, M. Quirynen, E. Schepers, J.L. Adams, D. van Steenberghe, Bone Formation following implantation of bone biomaterials into extraction sites, J. Periodontol. 79 (2008) 1108–1115, https://doi.org/10.1902/jop.2008.070476.
[104] F. Lambert, A. Leonard, G. Lecloux, S. Sourice, P. Pilet, E. Rompen, A comparison of three calcium phosphate–based space fillers in sinus elevation: a study in rabbits, Int. J. Oral Maxillofac. Implants 28 (2013) 393–402, https://doi.org/10.11607/jomi.2332.
[105] M. Tavoni, M. Dapporto, A. Tampieri, S. Sprio, Bioactive calcium phosphate-based composites for bone regeneration, J. Compos. Sci. 5 (2021) 227, https://doi.org/10.3390/jcs5090227.
[106] S. Samavedi, A.R. Whittington, A.S. Goldstein, Calcium phosphate ceramics in bone tissue engineering: a review of properties and their influence on cell behavior, Acta Biomater. 9 (2013) 8037–8045, https://doi.org/10.1016/j.actbio.2013.06.014.
[107] X.D. Zhu, H.J. Zhang, H.S. Fan, W. Li, X.D. Zhang, Effect of phase composition and microstructure of calcium phosphate ceramic particles on protein adsorption, Acta Biomater. 6 (2010) 1536–1541, https://doi.org/10.1016/j.actbio.2009.10.032.
[108] H. Ma, C. Feng, J. Chang, C. Wu, 3D-printed bioceramic scaffolds: from bone tissue engineering to tumor therapy, Acta Biomater. 79 (2018) 37–59, https://doi.org/10.1016/j.actbio.2018.08.026.
[109] A.A. Vu, D.A. Burke, A. Bandyopadhyay, S. Bose, Effects of surface area and topography on 3D printed tricalcium phosphate scaffolds for bone grafting applications, Addit. Manuf. 39 (2021) 101870, https://doi.org/10.1016/j.addma.2021.101870.
[110] C. Gao, S. Peng, P. Feng, C. Shuai, Bone biomaterials and interactions with stem cells, Bone Res 5 (2017) 17059, https://doi.org/10.1038/boneres.2017.59.
[111] M.J. Dewey, B.A.C. Harley, Biomaterial design strategies to address obstacles in craniomaxillofacial bone repair, RSC Adv. 11 (2021) 17809–17827, https://doi.org/10.1039/D1RA02557K.
[112] Q. Liu, W.F. Lu, W. Zhai, Toward stronger robocast calcium phosphate scaffolds for bone tissue engineering: a mini-review and meta-analysis, Biomater. Adv. 134 (2022) 112578, https://doi.org/10.1016/j.msec.2021.112578.
[113] T. Koizumi, Y. Komuro, Influence of mixing blood with calcium phosphate bone paste on hardening, J. Craniofac. Surg. 22 (2011) 329–332, https://doi.org/10.1097/SCS.0b013e3181f7df69.
[114] W. Thein-Han, J. Liu, H.H.K. Xu, Calcium phosphate cement with biofunctional agents and stem cell seeding for dental and craniofacial bone repair, Dent. Mater. 28 (2012) 1059–1070, https://doi.org/10.1016/j.dental.2012.06.009.
[115] B.T. Smith, M. Santoro, E.C. Grosfeld, S.R. Shah, J.J.J.P. Van Den Beucken, J. A. Jansen, A.G. Mikos, Incorporation of fast dissolving glucose porogens into an injectable calcium phosphate cement for bone tissue engineering, Acta Biomater. 50 (2017) 68–77, https://doi.org/10.1016/j.actbio.2016.12.024.
[116] C.I.A. Van Houdt, R.S. Preethanath, B.A.J.A. Van Oirschot, P.H.W. Zwarts, D.J. O. Ulrich, S. Anil, J.A. Jansen, J.J.J.P. Van Den Beucken, Toward accelerated bone regeneration by altering poly(d , l -lactic- *co* -glycolic) acid porogen content in calcium phosphate cement: bone Regeneration by Altering PLGA Porogen in Calcium Phosphate Cement, J. Biomed. Mater. Res. 104 (2016) 483–492, https://doi.org/10.1002/jbm.a.35584.
[117] A.-M. Yousefi, A review of calcium phosphate cements and acrylic bone cements as injectable materials for bone repair and implant fixation, J. Appl. Biomater. Funct. Mater. 17 (2019) 228080001987259, https://doi.org/10.1177/2280800019872594.
[118] E. Sadeghian Dehkord, G. Kerckhofs, P. Compère, F. Lambert, L. Geris, An empirical model linking physico-chemical biomaterial characteristics to intra-oral bone formation, J. Funct. Biomater. 14 (2023) 388, https://doi.org/10.3390/jfb14070388.
[119] B. Gaihre, S. Uswatta, A. Jayasuriya, Reconstruction of craniomaxillofacial bone defects using tissue-engineering strategies with injectable and non-injectable scaffolds, J. Funct. Biomater. 8 (2017) 49, https://doi.org/10.3390/jfb8040049.
[120] P. Janicki, G. Schmidmaier, What should be the characteristics of the ideal bone graft substitute? Combining scaffolds with growth factors and/or stem cells, Injury 42 (2011) S77–S81, https://doi.org/10.1016/j.injury.2011.06.014.
[121] G. Brunello, S. Panda, L. Schiavon, S. Sivolella, L. Biasetto, M. Del Fabbro, The impact of bioceramic scaffolds on bone regeneration in preclinical in vivo studies: a systematic review, Materials 13 (2020) 1500, https://doi.org/10.3390/ma13071500.
[122] C. Hayashi, A. Kinoshita, S. Oda, K. Mizutani, Y. Shirakata, I. Ishikawa, Injectable calcium phosphate bone cement provides favorable space and a scaffold for periodontal regeneration in dogs, J. Periodontol. 77 (2006) 940–946, https://doi.org/10.1902/jop.2006.050283.
[123] Y. Shirakata, T. Yoshimoto, H. Goto, Y. Yonamine, H. Kadomatsu, M. Miyamoto, T. Nakamura, C. Hayashi, Y. Izumi, Favorable periodontal healing of 1-wall infrabony defects after application of calcium phosphate cement wall alone or in combination with enamel matrix derivative: a pilot study with canine mandibles, J. Periodontol. 78 (2007) 889–898, https://doi.org/10.1902/jop.2007.060353.
[124] Y. Shirakata, T. Setoguchi, M. Machigashira, T. Matsuyama, Y. Furuichi, K. Hasegawa, T. Yoshimoto, Y. Izumi, Comparison of injectable calcium phosphate bone cement grafting and open flap debridement in periodontal intrabony defects: a randomized clinical trial, J. Periodontol. 79 (2008) 25–32, https://doi.org/10.1902/jop.2008.070141.
[125] J. Lammens, M. Maréchal, H. Delport, L. Geris, H. Oppermann, S. Vukicevic, F. P. Luyten, A cell-based combination product for the repair of large bone defects, Bone 138 (2020) 115511, https://doi.org/10.1016/j.bone.2020.115511.